


REVIEW

Open Access



# Recent advances in the development of engineered biochar for CO<sub>2</sub> adsorption: Research on heteroatom-doped biochar

Xiangping Li<sup>1\*</sup>, Xuanxuan Li<sup>1†</sup>, Caixia Zhang<sup>1</sup>, Yifei Yu<sup>1</sup>, Qing Liu<sup>1</sup>, Mahesh Hordagoda<sup>2</sup>, Wenbing Ding<sup>1</sup>, Shengshu Xu<sup>1</sup>, Thilini U. Ariyadasa<sup>3</sup>, P. H. V. Nimarshana<sup>2</sup>, Xizhuang Qin<sup>1</sup> and Peng Liang<sup>1\*</sup>

## Abstract

With rising atmospheric CO<sub>2</sub> levels driving global warming, carbon capture and storage (CCS) technologies are critical. Biochar, an eco-friendly and cost-effective carbon material, has gained attention for low-temperature CO<sub>2</sub> capture due to its sustainable adsorption properties. However, raw biochar's limited pore structure and surface chemistry hinder its efficiency. Among modification strategies, heteroatom doping is particularly effective. By enriching functional groups and tuning the carbon framework, this approach significantly improves CO<sub>2</sub> capture performance. This review explores recent advancements in the development of engineered biochar for CO<sub>2</sub> adsorption, with a focus on heteroatom doping techniques. Additionally, key quantitative performance metrics were compiled and compared, including adsorption capacities and isosteric heats of adsorption ( $Q_{st}$ ) (and, where available, selectivity/working capacity), to quantify how different doping strategies alter gas uptake and binding strength and to establish structure-performance relationships. Among various dopants (such as nitrogen, sulfur, phosphorus, and boron), nitrogen doping has attracted much attention due to its significant enhancement in the ability to capture CO<sub>2</sub>. This is mainly because nitrogen atoms can more effectively regulate the electronic structure and pore structure of the material in a coordinated manner, thereby enhancing the dual effects of physical and chemical adsorption on CO<sub>2</sub>. A critical comparison is made between pre-modification doping (incorporating heteroatoms during biomass carbonization) and post-modification doping (treating already-formed biochar), revealing that pre-modification generally offers superior doping efficiency and structural stability. Moreover, the review examines co-doping strategies, where synergistic effects between multiple elements, as exemplified by nitrogen-phosphorus co-doping or nitrogen-sulfur co-doping of biochar, further optimize the adsorption capacity. Finally, critical barriers to industrialization, including techno-economic feasibility and regeneration energy costs, are discussed. Future perspectives emphasize the integration of machine learning for rational design, standardized characterization protocols, and life-cycle assessments (LCA) to accelerate the deployment of biochar in practical CCUS applications. The review highlights the mechanisms of CO<sub>2</sub> capture, emphasizing the balance between physical adsorption and chemisorption. The challenges for development of engineered biochar for CO<sub>2</sub> capture are prospected. Further research on improving chemical adsorption performance while preserving physical adsorption properties is still required to improve biochar's application in sustainable CO<sub>2</sub> capture technologies.

<sup>†</sup>Xiangping Li and Xuanxuan Li contributed equally to this work.

\*Correspondence:

Xiangping Li  
lixpln@sdust.edu.cn

Peng Liang  
liangpeng202@hotmail.com

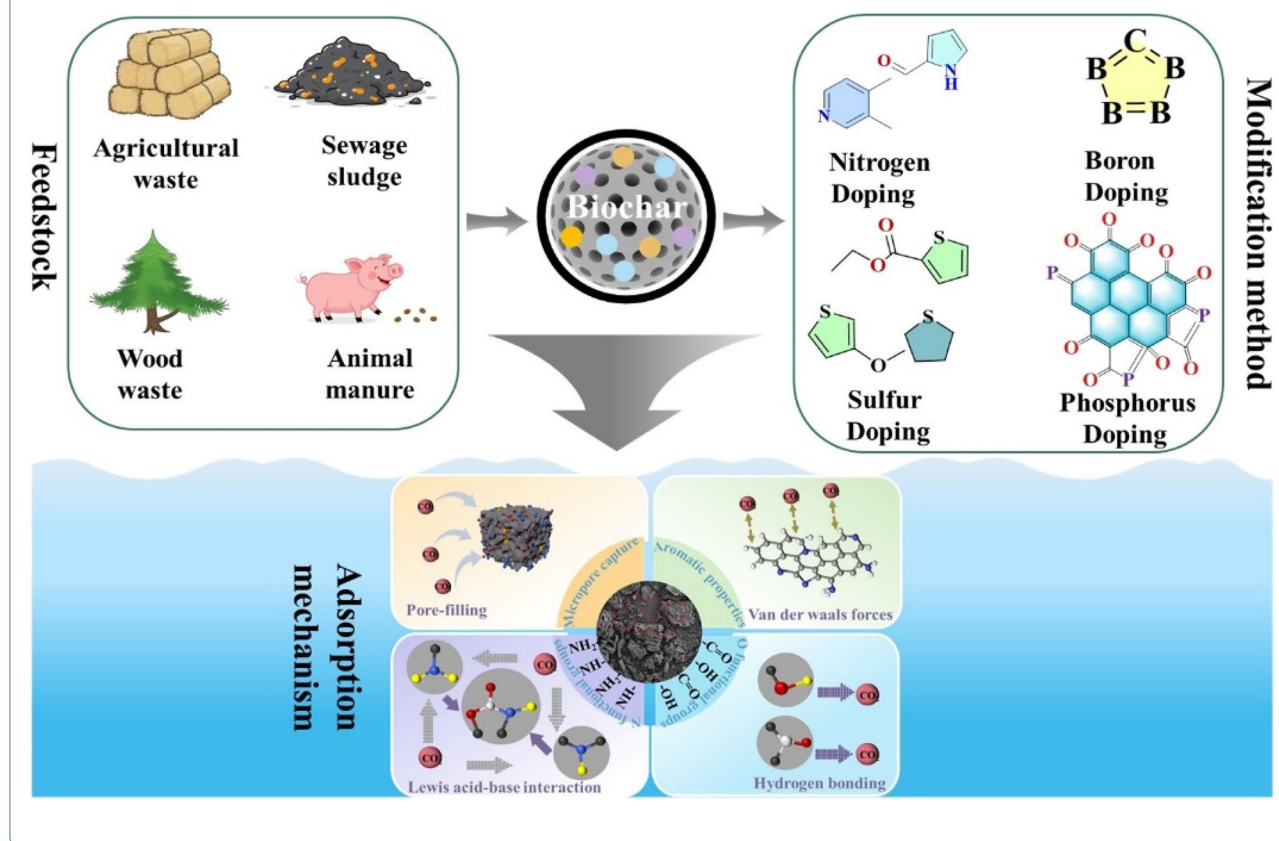
Full list of author information is available at the end of the article

## Highlights

- Recent advances of engineered and modified biochar for CO<sub>2</sub> capture were reviewed.
- Tuning physicochemical properties to enhance CO<sub>2</sub> capture of biochar were discussed.
- Different modification approaches of biochar were reviewed.
- The heteroatoms and doping methods of biochar on CO<sub>2</sub> capture were analyzed.
- The mechanisms of modified biochar on CO<sub>2</sub> adsorption were summarized and discussed.

**Keywords** CO<sub>2</sub> adsorption, Biochar, Heteroatom doping, Physical activation, Chemical activation

## Graphical Abstract



## 1 Introduction

Climate change over the past two centuries has been driven by both human activities and natural factors, leading to global warming and frequent extreme weather events (Donger et al. 2025). The industrial revolution and continuous fossil fuel combustion have significantly increased atmospheric CO<sub>2</sub> concentrations (Sánta and Garbai 2025), reaching 419 ppm in 2024—50% higher than in the 18th century (Fig. 1a), with coal combustion being the dominant contributor (Fig. 1b). The United Nations Intergovernmental Panel on Climate Change (UN IPCC)

projects—that atmospheric CO<sub>2</sub> concentrations will rise to around 570 ppm by 2100 (Liang and Zhou 2024). Excessive CO<sub>2</sub> emissions are thus the principal cause of global warming and climate anomalies (Wang et al. 2024c), highlighting the urgent need for mitigation strategies.

The conversion of CO<sub>2</sub> into valuable products such as fuels, polymers, and chemicals can recycle carbon resources and reduce environmental impacts (Ji et al. 2022). Although CO<sub>2</sub> capture, utilization, and storage (CCUS) technologies provide mature and cost-effective solutions that mitigate climate change impacts and

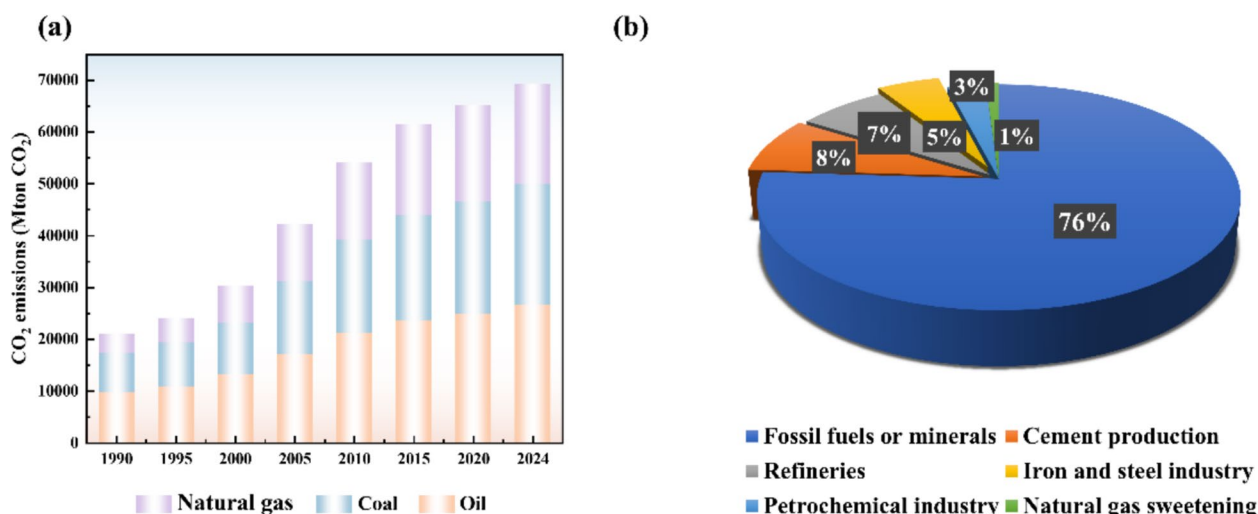


**Fig. 1** a Global CO<sub>2</sub> emissions in 1990–2024, and **b** contribution of each CO<sub>2</sub> emission source. Adapted from Shafawi et al. (2021). Copyright 2021 Elsevier

offer substantial economic benefits (Osman et al. 2021; Sai Bhargava Reddy et al. 2021), the capture process remains the most energy-intensive and costly component. Current research primarily focuses on CO<sub>2</sub> capture, purification, and adsorbent preparation. CO<sub>2</sub> capture technologies are divided into pre-combustion, total oxygen combustion, and post-combustion capture (Fig. 2). Post-combustion capture offers compatibility with existing emission control systems and reduced technical risk (Cui 2022; Gao et al. 2020). However, methods such as chemical absorption and solvent absorption among them face long-term application challenges such as high energy consumption and equipment corrosion (Lu et al. 2023). Solid adsorbent-based CO<sub>2</sub> capture provides an alternative with broader temperature tolerance and lower regeneration energy (Portillo et al. 2019). An ideal CO<sub>2</sub> adsorbent should possess a high adsorption capacity and selectivity, rapid kinetics, stability, and low production cost for large-scale application. Various adsorbents have been extensively studied, such as metal–organic frameworks (MOFs), metal oxides, zeolites, activated carbon, mesoporous carbon, ion exchange resins, and carbon nanomaterials (Cui 2022). However, despite their superior CO<sub>2</sub> adsorption properties, these materials face significant challenges in terms of cost, scalability, and sustainability, which limit their large-scale application. For instance, while MOFs exhibit high efficiency under high-pressure conditions, their high production costs make large-scale application challenging (Lee et al. 2024; Yang et al. 2025). Zeolites, although highly selective, perform poorly in humid conditions (Abd et al. 2020; Jiang et al. 2024). Activated carbon, despite its enhanced adsorption capacity due to oxidized surfaces, still struggles with

CO<sub>2</sub>/N<sub>2</sub> selectivity (Llamas et al. 2021). In comparison, metal oxides like calcium oxide suffer from reduced efficiency after multiple cycles. Table 1 provides a comparison of the performance of various physical adsorbents for CO<sub>2</sub> capture, as reported in numerous review articles (Abd et al. 2020; Elhenawy et al. 2020; Osman et al. 2021).

These limitations highlight the urgent need for developing adsorbents that integrate efficiency, cost-effectiveness, and sustainability. In this context, biochar offers a unique solution. Biochar is a carbon-based product derived from abundant biomass resources, such as lignocellulosic residues and organic waste, through cost-effective thermochemical methods (Khoshraftar and Ghaemi 2022). It shows potential for diverse applications in agriculture (improving soil fertility and reducing greenhouse gas emissions), climate change mitigation (adsorbing pollutants like NO<sub>x</sub>, SO<sub>x</sub>, H<sub>2</sub>S, and greenhouse gases), environmental remediation (removing pollutants, heavy metals, nitrogen, and phosphorus), and materials science (developing materials for catalysts, building materials, and batteries) (Dai et al. 2019; Dissanayake et al. 2020; Khandaker et al. 2020; Liu et al. 2019b), as illustrated in Fig. 3. More importantly, its production process is more economical and environmentally friendly compared to conventional synthetic materials (Khoshraftar et al. 2023). Through engineered design, biochar's adsorption performance can be enhanced, providing a distinct advantage in creating economical, efficient, and sustainable carbon capture solutions. From an engineering perspective, engineered biochar also shows strong potential for large-scale deployment at both the adsorption reactor and system levels. Owing to its high mechanical stability, tunable particle size, and resistance to thermal and

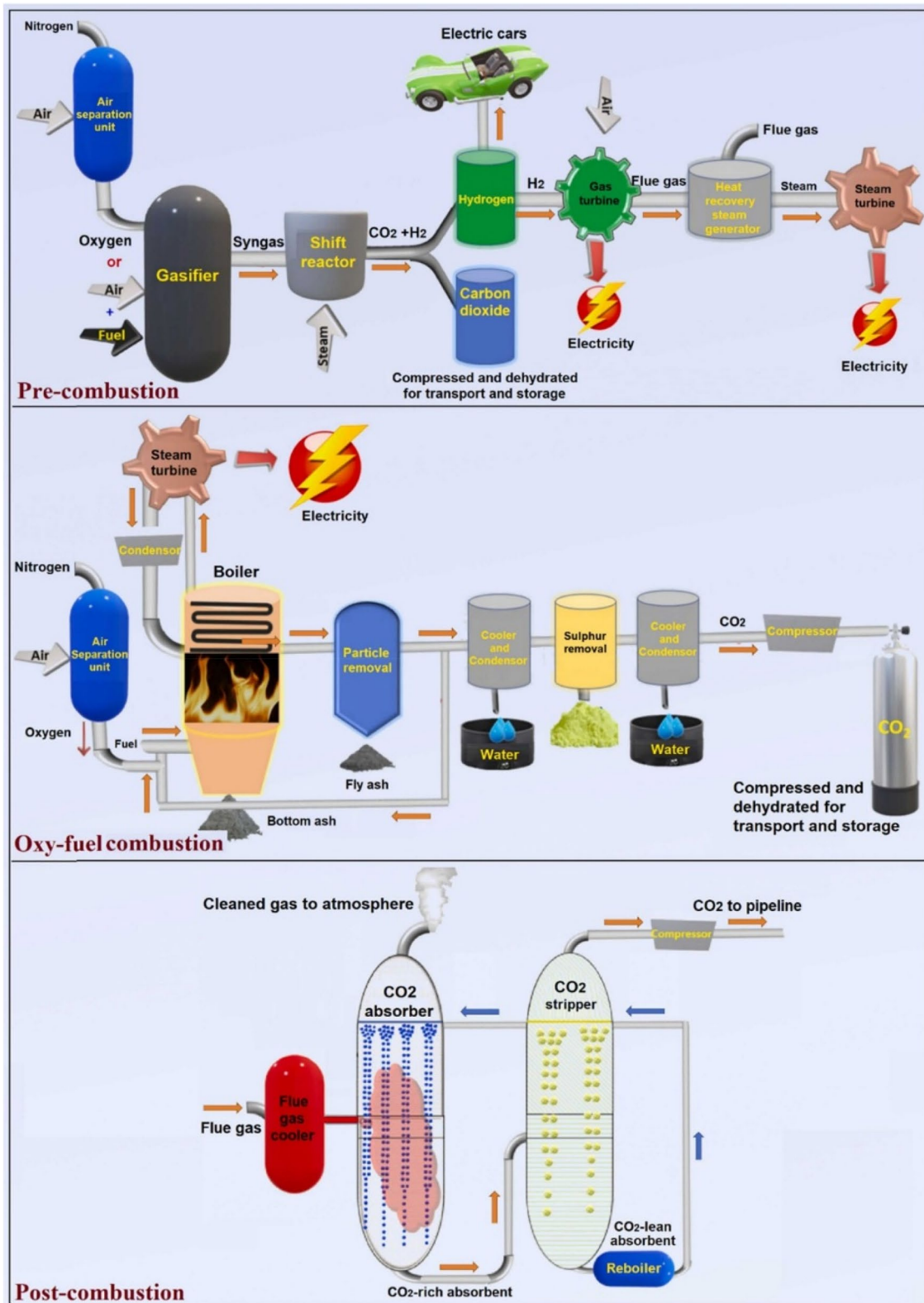
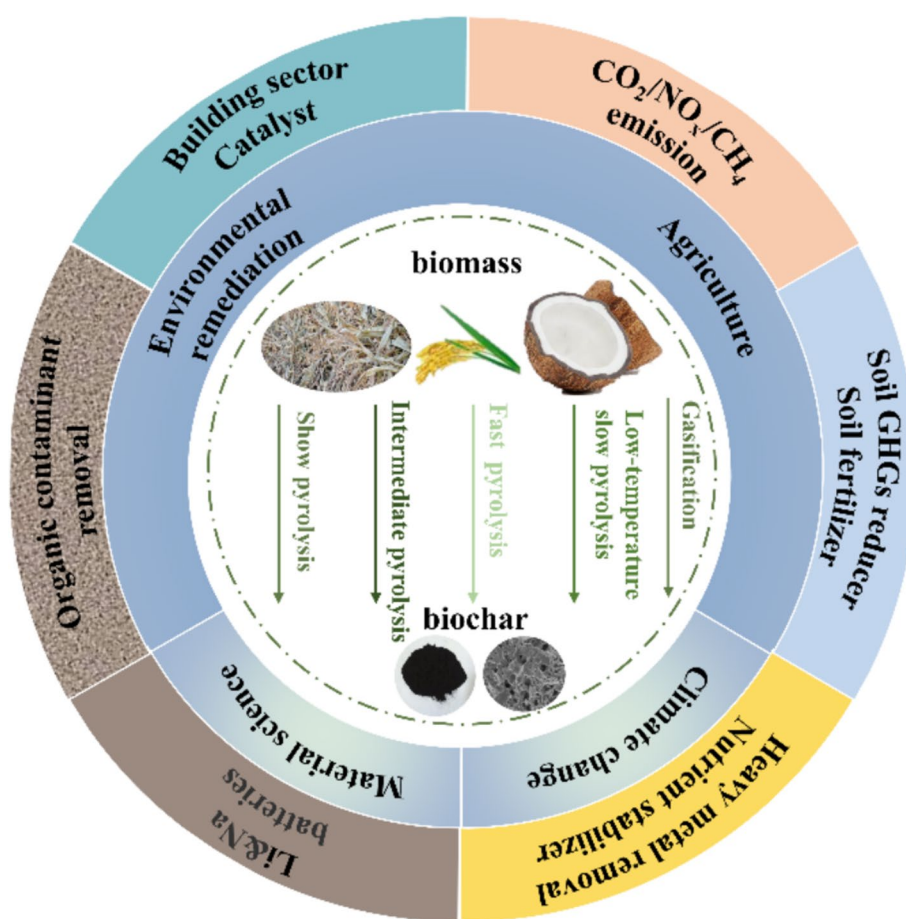


Fig. 2 Diagram of CO<sub>2</sub> capture technologies (Shafawi et al. 2021). Copyright 2021 Elsevier

**Table 1** A selection of physical solid adsorbents utilized for CO<sub>2</sub> capture (Ahmed et al. 2016; León et al. 2020; Ruen-ngam et al. 2009)

Solid adsorbent	Activated carbons	Zeolites	MOFs
Optimal operating temperature (°C)	25–75	< 100	–78 to +80
Optimal operating pressure (psi)	1.45–145	1.45–145	1.4–440
Primary application in gas separation	CO <sub>2</sub> /CH <sub>4</sub>	CO <sub>2</sub> /N <sub>2</sub>	CO <sub>2</sub> /CH <sub>4</sub> , CO <sub>2</sub> /H <sub>2</sub>
CO <sub>2</sub> selectivity	Medium	Low	High
CO <sub>2</sub> adsorption capacity	Higher than zeolite at high pressures, which decreases at low pressure	Medium	High
Stability under humid conditions	Stable	Unstable	Unstable
Synthesis cost	\$ 2.15/kg	\$ 40–96/Kg	~\$ 200/kg (MOF-5) and \$130/kg (MOF-177)



**Fig. 3** The diverse utilization of biochar across various domains. Adapted from Shafawi et al. (2021). Copyright 2021 Elsevier

chemical degradation, engineered biochar can be readily integrated into fixed-bed, packed-bed, and fluidized-bed adsorption reactors commonly used in post-combustion CO<sub>2</sub> capture. In addition, its relatively low regeneration temperature and good cyclic stability enable energy-efficient operation in continuous adsorption–desorption

systems, offering advantages in terms of operational cost, scalability, and compatibility with existing industrial infrastructure.

Biochar has been extensively studied over the past few decades. However, there are still significant gaps in its production, activation and application, which restrict its

large-scale application. Therefore, establishing a full-chain research framework encompassing feedstock selection-targeted preparation-functional modification-multi-field applications is essential for unlocking its potential as a high-performance adsorbent. Biochar activation and modification remain key bottlenecks restricting its broader implementation. Physical and chemical activation strategies enhance pore development and surface functionality (Li and Xiao 2019; Zubbri et al. 2020), but recent research has increasingly emphasized structural precision through heteroatom doping. Heteroatoms such as N, S, P and B form unique chemical structures within the carbon matrix (Jang et al. 2019), improving surface polarity, functional groups, and active sites, thereby significantly enhancing CO<sub>2</sub> adsorption through mechanisms such as stronger acid–base interactions and improved micropore utilization (Fang et al. 2023; Sun et al. 2023a). Studies reported in the original text show substantial increases in adsorption capacity and selectivity after doping, underscoring its practical efficacy. At the application stage, fully optimized biochar demonstrates outstanding adsorption and environmental capabilities: in water treatment, it efficiently removes antibiotics (e.g., sulfamethazine) and organic dyes; in climate mitigation, it serves as a highly competitive and low-cost CO<sub>2</sub> sorbent through mechanisms such as micropore filling, hydrogen bonding, and acid–base interactions (Guo et al. 2022; Sun et al. 2025). Despite these advancements, a comprehensive understanding of how different heteroatoms, doping pathways, and synergistic activation strategies influence CO<sub>2</sub> capture remains incomplete. Therefore, this review focuses on the latest progress in heteroatom-doped biochar for CO<sub>2</sub> adsorption, emphasizing synthesis strategies, adsorption mechanisms, and future challenges. By establishing a detailed framework that links biomass resources, engineered preparation, functional modification, and multi-field applications, this work aims to identify key limitations and outline pathways toward developing high-performance, scalable, and sustainable CO<sub>2</sub> adsorbents, and to provide an economic and sustainable solution for environmental pollution control and resource recovery.

## 2 Properties analysis of biochar

### 2.1 Physical properties

Biochar is predominantly composed of elements such as C, O, H, N, K, Ca, Na, Mg, among others (Li et al. 2026, 2024a). The carbon predominantly manifests in the form of aromatic rings, whereas K, Na, Ca, and Mg are typically present in the ash as carbonates, phosphates, or oxides. The relative proportions of these elements exhibit considerable variation based on the feedstock, thereby influencing the properties of the resultant biochar. As the pyrolysis temperature escalates, a more comprehensive

transformation of the organic components in the biomass occurs, resulting in an increase in C and ash content, and a decrease in H, O, and N content. This reduction in H and O content significantly lowers the oxygen-to-carbon (O/C) ratio, a critical determinant of hydrophobicity. The reduced O/C ratio enhances the biochar's hydrophobicity, thereby boosting its adsorption capacity for non-polar molecules like CO<sub>2</sub>. Specifically, the elimination of polar oxygen-containing functional groups (e.g., hydroxyl and carboxyl) diminishes the capacity of the biochar surface to form hydrogen bonds with water molecules. Consequently, this shift in surface chemistry, quantitatively reflected by lower O/C ratios, directly correlates with a transition from hydrophilicity to enhanced hydrophobicity, thereby minimizing competitive water vapor adsorption under humid conditions.

During pyrolysis, volatile substances in biomass are released, resulting in high-porosity biochar characterized by a diverse pore structure and low density. The specific surface area and pore size are pivotal for CO<sub>2</sub> adsorption. Research has demonstrated a direct correlation between surface area and CO<sub>2</sub> adsorption capacity, as CO<sub>2</sub> adsorption is primarily physical. A larger surface area offers more active sites for adsorption. The pores formed during pyrolysis include nanopores (<0.9 nm), micropores (<2 nm), mesopores (2–50 nm), and macropores (>50 nm). Notably, micropores, especially ultramicropores (<0.7 nm), are instrumental in CO<sub>2</sub> adsorption due to their size being comparable to the kinetic diameter of CO<sub>2</sub> molecules, which enhances van der Waals interactions and increases the probability of molecular sieving effect. The pore range optimally maximizes interaction efficiency at a molecular level and selectively traps CO<sub>2</sub> molecules by limiting the movement of larger gas molecules. At the same time, it is also affected by temperature and pressure. At 25 °C and 0 °C, CO<sub>2</sub> adsorption is predominantly in pores smaller than 1 nm, whereas for pressures up to 100 kPa, CO<sub>2</sub> adsorption is controlled by 1 nm micropores (Tang et al. 2024). Table 2 presents the specific surface area and pore size distribution of different types of biochar. It is evident that cellulose-based biochars (e.g., straw, shells, and wood) exhibit notably higher surface areas than non-cellulose-based biochars (e.g., manure and sludge). This can be attributed to the inherent rich pore structure of cellulose-based biomass. As pyrolysis temperature increases, the release of volatile substances augments the pore size and surface area of the biochar (Cao et al. 2022). Nevertheless, excessive temperatures can damage the micropore structure, diminishing the surface area and leading to pore obstruction. Studies have reported that micropore collapse or shrinkage tends to occur when pyrolysis temperatures exceed a typical threshold of approximately 700–800 °C, depending on

**Table 2** Specific surface area and pore size distribution of different types of biochar

Biochar sample		Temperature/°C	Surface area/(m <sup>2</sup> /g)	Total pore volume/(cm <sup>3</sup> /g)	Average pore size/nm	Ref.
Straw	Corn straw	300–700	1.56–316.00	0.002–0.007	1.56–37.66	(Wang et al. 2022a)
	Wheat straw	200–600	1.72–512.29	0.0386–0.1032	2.31–18.63	(Yan et al. 2022)
	Rice straw	300–700	4.21–13.13	0.007–0.026	1.54–13.38	(Cao et al. 2022)
	Rape straw	450–650	37.58–68.07	0.095–0.261	3.93–9.17	(Wang et al. 2024b)
Shell	Peanut shell	300–600	1.63–355.70	0.008–0.0494	2.69–3.82	(Wang et al. 2020a)
	Rice husk	300–1046	1.39–377.72	0.0001–0.006	14.56–50.00	(Huong et al. 2020; Singh Karam et al. 2022)
Wood	Rhus vernicifera	300–550	2.38–229.43	0.0001–0.006	10.72–17.79	(Yu et al. 2023)
	Charcoal	300–600	1.63–21.03	0.004367–0.04096	12.36–16.38	(Li et al. 2024b)
Manure	Pig manure	400–600	5.17–10.56	0.0130–0.0440	12.36–16.38	(Yang et al. 2023)
	Cow dung	300–700	1.55–31.23	0.0026–0.0234	3.00–7.34	(Yang et al. 2023)
Sludge	Pharmaceutical sludge	500–900	9.46–264.05	0.014–0.330	2.27–5.93	(Wu et al. 2022a)
	Pharmaceutical sludge	300–900	4.00–67.60	0.0537–0.0986	3.74–3.84	(Rangabhashiyam et al. 2022)

biomass type and heating conditions. Therefore, meticulous regulation of biochar porosity is essential for amplifying CO<sub>2</sub> adsorption capacity.

## 2.2 Chemical properties

The surface chemical properties of biochar have a significant impact on CO<sub>2</sub> adsorption, owing primarily to the presence of diverse functional groups, such as carboxyl, hydroxyl, amine, amide, and lactone groups. These functional groups influence both the adsorptivity and hydrophilicity of biochar. Surface functional groups of biochar, such as -COO<sup>-</sup>, -OH, and -COOH, can adsorb H<sup>+</sup> (Dong et al. 2025), thereby improving soil pH. Additionally, ether groups and aromatic rings can interact with heavy metals to limit their migration. As CO<sub>2</sub> is acidic, it can react with alkaline groups in biochar, such as nitrogenous functional groups, and can engage hydrogen bonding and nucleophilic interactions with -OH, -COOH, and other oxygenated groups (Zhang et al. 2025c). However, acidic groups such as carboxylic acids, phenols and lactones have a poor effect on CO<sub>2</sub> adsorption. High pyrolysis temperatures (100–700 °C) induce the dissociation of these acidic groups into CO and CO<sub>2</sub> (Fig. 4a), rendering biochar more conducive for CO<sub>2</sub> adsorption. Notably, although pyridone, chromene, and ketones have limited alkalinity, they are considered alkaline groups (Fig. 4b) (Dissanayake et al. 2020) and exhibit stability at elevated temperatures. In general, pyrolysis temperature strongly affects the elemental composition of biochar. As temperature escalates, the carbon content increases, whereas the contents of H, O, and N diminish due to the loss of OH groups and dehydration. Nitrogenous functional groups, such as amino groups, undergo removal above 400 °C

during biomass pyrolysis. Biochar retains stable amino groups within its aromatic structure, but further activation is imperative to incorporate nitrogenous groups. The expulsion of water, CO<sub>2</sub>, CO, hydrocarbons, and tar vapors during carbonization additionally diminishes the contents of H, O, and N (Ali et al. 2025). The decline in H and C elements at elevated temperatures might be due to the cleavage of weak bonds within the carbon matrix (Table 3; Beljin et al. 2024; Sierra-Jimenez et al. 2025).

The surface charge of biochar depends on the functional groups. These groups can be divided into two categories: electron donors such as OH, NH<sub>2</sub>, O(C=O)R, and electron acceptors such as (C=O)H, NO<sub>2</sub>, (C=O)OH). Owing to these functional groups, biochar surfaces exhibit a variety of acidic and basic sites, such as weakly acidic phenolic and carbonyl groups, strong Brønsted acids (e.g., carboxyl groups), and basic pyridone groups and chromene groups (Kazemi Shariat Panahi et al. 2020). Predominantly, biochar surfaces exhibit a negative charge, rendering them apt for CO<sub>2</sub> capture.

The quantity of functional groups varies according to the type of biomass and the method of preparation, with non-cellulosic biochar demonstrating a greater number of nitrogen- and sulfur-containing groups (Luo et al. 2023). Hydrophobicity and non-polarity enhance CO<sub>2</sub> adsorption by reducing competition from H<sub>2</sub>O molecules. The ratios of H/C, O/C, and (O+N)/C serve as indicators for aromaticity, hydrophobicity, and polarity, respectively. Low O/C and H/C ratios, coupled with high aromaticity, signify pronounced hydrophobicity, which augments CO<sub>2</sub> adsorption. Carbonization reduces the O, H, N, and S content, thus diminishing the polarity of biochar. This reduction limits the competition for adsorption

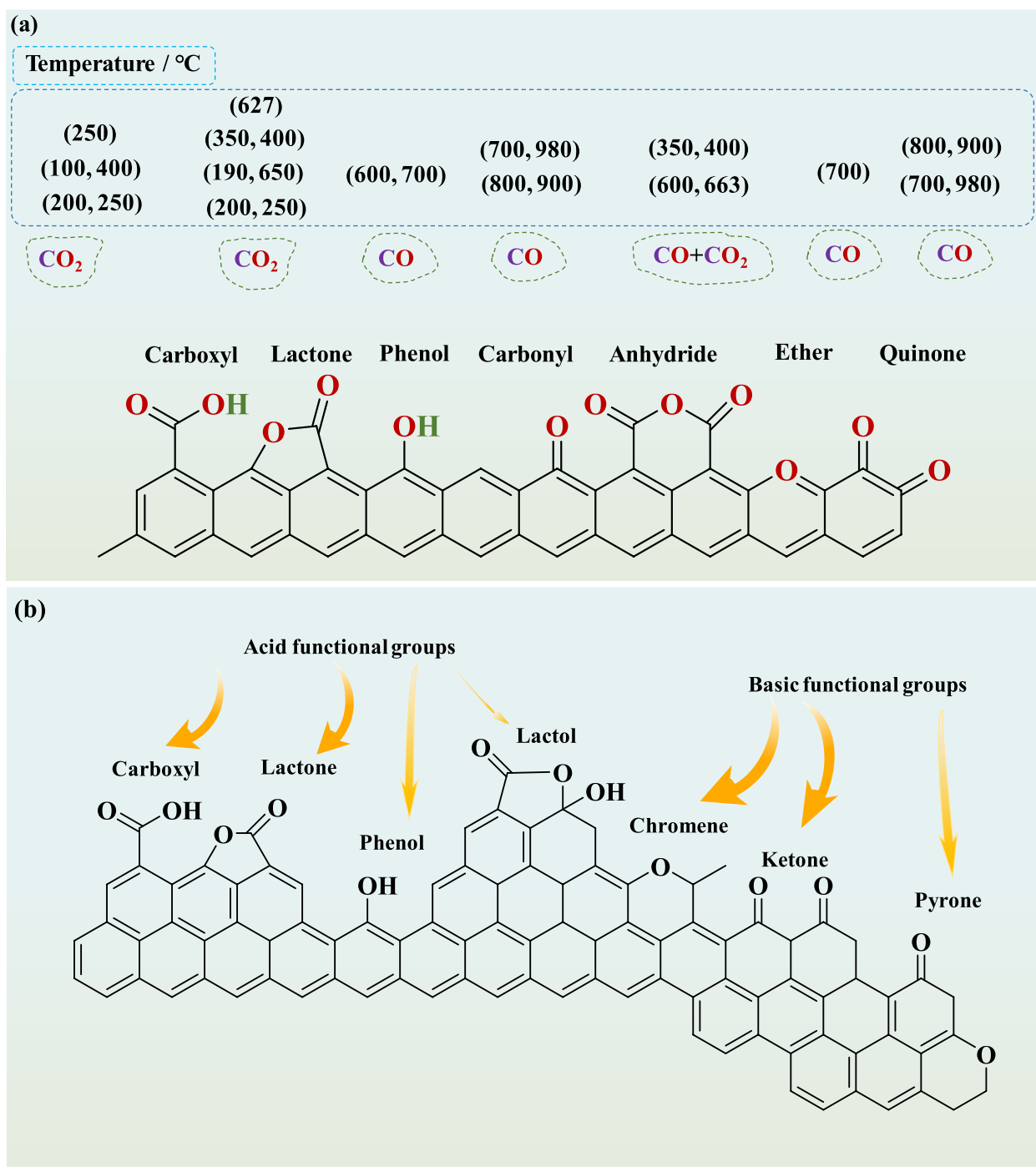


**Fig. 4** **a** Surface oxygen-containing groups and their subsequent decomposition as analyzed by TPD. Copyright 2022 Springer. Adapted from Amer et al. (2024a) and **b** acidic and basic O-containing functional groups present in biochar. Adapted from Montes-Morán et al. (2004). Copyright 2004 Elsevier

with polar molecules, subsequently promoting CO<sub>2</sub> adsorption. Studies have shown that higher temperatures eliminate polar functional groups, thereby enhancing hydrophobicity and aromaticity. This improvement leads to an increase in CO<sub>2</sub> adsorption capacity. Biochar

that has been activated with KOH retains a variety of surface functional groups, providing the requisite acidic or alkaline characteristics to the biochar surface. These characteristics are essential for effective CO<sub>2</sub> adsorption (Zubbri et al. 2021).

**Table 3** The impact of pyrolysis temperature on the properties of pristine biochar derived from diverse biomass feedstocks

Feedstock	Pyrolysis temperature (°C)	C (%)	H (%)	N (%)	O (%)	BET surface area (m <sup>2</sup> /g)	Total pore volume (cm <sup>3</sup> /g)	Micropores volume (cm <sup>3</sup> /g)	Ref.
Rambutan peel	500	76.36	2.90	1.35	19.22	7.80	0.011	0.002	(Zubbri et al. 2021)
	700	81.64	1.37	1.00	15.93	175.84	0.111	0.066	
	900	83.38	0.90	0.77	14.71	569.64	0.313	0.201	
Walnut shell	500	69.42	3.85	1.54	25.07	94.509	0.054	0.021	(Lahijani et al. 2018)
	700	80.35	1.61	0.41	17.54	246.991	0.141	0.104	
	900	84.86	1.16	0.34	13.63	397.015	0.198	0.159	
Date palms	300	63.65	3.82	1.01	18.78	2.040	0.0057	-	(Elnour et al. 2019)
	400	64.95	2.96	0.89	17.04	5.535	0.0055	-	
	500	70.75	2.33	0.86	9.85	123.625	0.0209	-	
Peanut shell	600	74.76	1.60	0.71	7.31	221.230	0.0371	-	(Gai et al. 2014)
	700	72.76	0.9	0.61	5.32	249.130	0.0308	-	
	400	58.4	1.5	1.8	21.0	3.0	0.007	-	
Vegetable waste	500	64.5	3.5	1.7	18.5	5.0	0.022	-	(Igalavithana et al. 2017)
	600	71.9	2.8	1.6	15.0	28.0	0.11	-	
	700	74.4	2	1.4	14.2	195.0	0.033	-	
Pine cone	200	52.89	6.9	4.2	36.02	0.36	0.00259	-	(Gai et al. 2014)
	500	74.71	3.08	5.41	16.01	1.16	0.00242	-	
	200	69.74	2.13	1.03	27.09	0.47	0.00238	-	
Wheat straw	500	74.64	2.62	1.81	20.94	192.97	0.0102	-	(Gai et al. 2014)
	400	57.8	3.2	1.5	21.6	5.5	0.012	-	
	500	70.3	2.9	1.4	17.7	10.0	0.09	-	
Corn straw	600	74.3	2.1	1.4	14.9	111.0	0.11	-	(Gai et al. 2014)
	700	73.9	4.3	1.2	14.6	177.0	0.058	-	
	400	56.1	1.3	2.4	22.0	4.0	0.008	-	
Miscanthus	500	58.0	2.7	2.3	21.5	6.0	0.012	-	(Chatterjee et al. 2020)
	600	58.6	2.0	2.0	18.7	7.0	0.012	-	
	700	59.5	1.5	1.6	16.6	3.0	0.006	-	
Switchgrass	500	74.60	3.38	0.45	17.42	168	0.08	-	(Chatterjee et al. 2020)
	600	82.35	2.32	0.35	11.22	345	0.18	-	
	700	83.69	2.40	0.29	8.20	368	0.18	-	
Corn stover	800	84.47	2.28	0.30	7.61	390	0.20	-	(Chatterjee et al. 2020)
	500	67.83	3.28	1.01	16.32	162	0.08	-	
	600	77.00	2.04	0.57	9.68	325	0.15	-	

### 3 Mechanisms of CO<sub>2</sub> capture by biochar

CO<sub>2</sub> adsorption by biochar involves multiple interaction mechanisms (Fig. 5a). These include physical processes driven by van der Waals forces and micropore filling, as well as chemical interactions such as hydrogen bonding and Lewis acid–base reactions facilitated by O and N functional groups.

From a quantitative perspective, the physical adsorption and micropore-filling behavior of CO<sub>2</sub> on biochar surfaces can be effectively described using adsorption isotherm models such as the Langmuir and Freundlich equations. The Langmuir model describes monolayer adsorption on homogeneous surfaces, while the

Freundlich model applies to multilayer adsorption on heterogeneous surfaces, which are widely applied to evaluate adsorption capacity, surface heterogeneity, and adsorption affinity in porous carbonaceous materials (Khoshraftar and Ghaemi 2024). CO<sub>2</sub> adsorption is influenced by factors such as the V<sub>n</sub> value, nitrogen content, and pore size distribution. Gaseous CO<sub>2</sub> molecules primarily rely on micropore adsorption, and smaller micropore sizes may help enhance CO<sub>2</sub> adsorption performance. The highly developed micropores in activated carbon continuously adsorb CO<sub>2</sub> until saturation, while mesoporous channels decrease mass transfer resistance, thereby improving micropore efficiency. From a

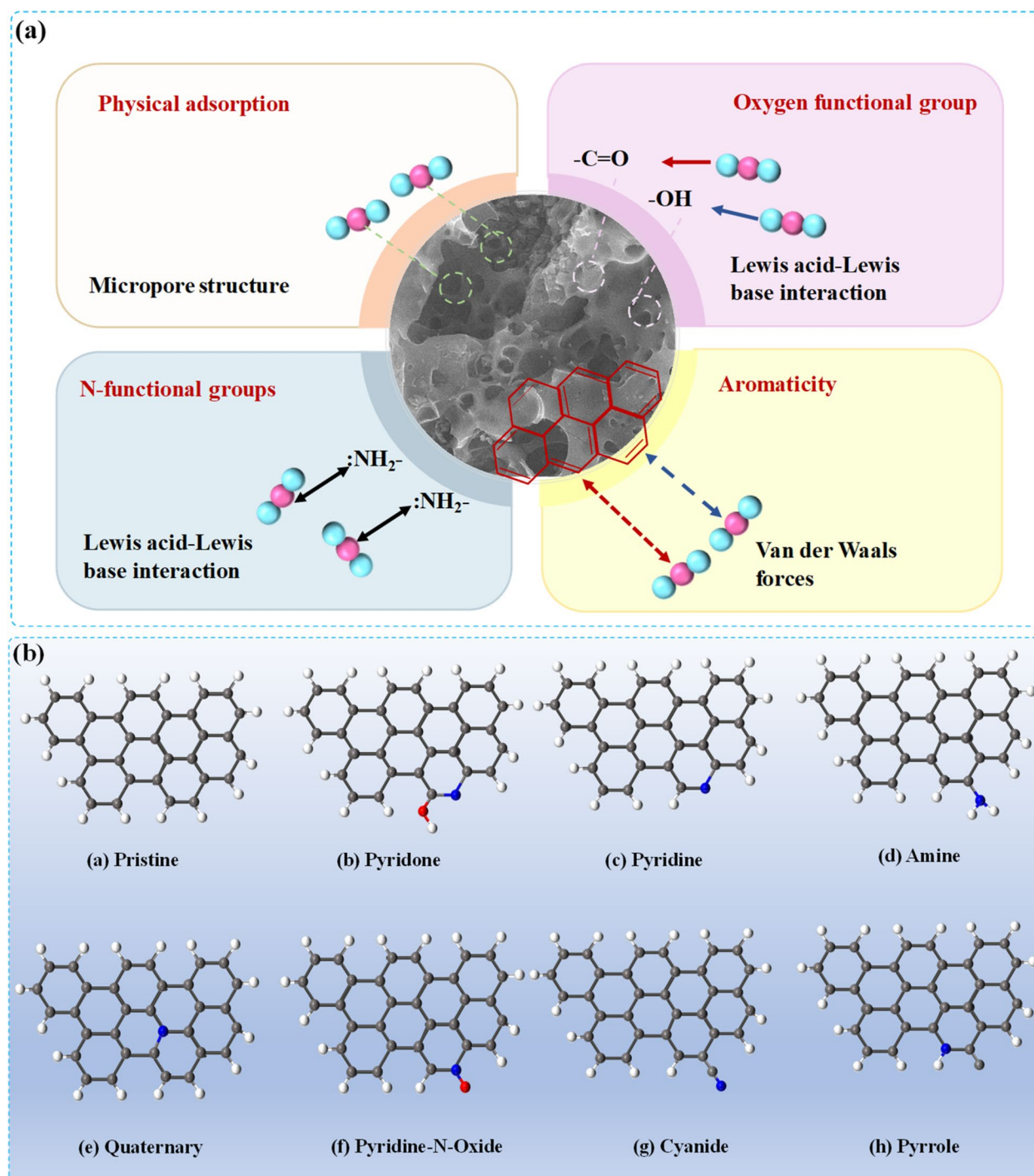


**Fig. 5** **a** Potential mechanisms underlying  $CO_2$  adsorption by biochar, and **b** Representations of nitrogenous functional groups, modeled using DFT. Atom color coding: C in gray, H in white, O in red, and N in blue. Adapted from Lim et al. (2016). Copyright 2016 ACS

kinetic standpoint (e.g., the analysis based on the particle internal diffusion model), the presence of mesopores facilitates gas diffusion and reduces intraparticle diffusion resistance, promoting faster  $CO_2$  transport to microporous adsorption sites and enhancing overall adsorption

efficiency. An effective activated carbon should possess an abundant surface area and functional groups, particularly oxygen-containing groups, which may facilitate interactions between the adsorbent and adsorbate via hydrogen bonding. However, acidic oxygen groups such

as carboxylic, phenolic, and lactonic groups, can impede CO<sub>2</sub> adsorption; their presence not only diminishes the surface basicity required for effective Lewis acid–base interactions with acidic CO<sub>2</sub> but also enhances hydrophilicity, thereby intensifying competitive adsorption by forming preferential hydrogen bonds with water molecules (Gao et al. 2025). Nitrogen groups such as amino and imino, due to their alkalinity and the presence of lone electron pairs in their structure, exhibit a higher affinity for CO<sub>2</sub>, thereby augmenting CO<sub>2</sub> chemisorption. Microporous materials, particularly those with pyrrole-N and pyridine-N groups, are more conducive for CO<sub>2</sub> capture at low temperatures. Zhang et al. (2025a) found that the synergistic effect of nitrogen content and narrow micropores influences CO<sub>2</sub> adsorption, while Wu et al. (2024b) noted that the selectivity of the samples mirrored the order of nitrogen content, indicating that nitrogen also augments selectivity. When pyrolysis temperature exceeds 400 °C, most nitrogen functional groups are lost, leaving only the pyridine groups that maintain their aromatic structure. Therefore, chemical modification using nitrogen-rich precursors is necessary to introduce basic nitrogen functional groups. Notable nitrogen functional groups include pyridone, pyridine, pyridine-n-oxide, pyrrole, amine, quaternium-N, and cyanide groups (Fig. 5b). These groups differ in their alkaline strengths, with pyridone, pyridine, and pyrrole being the most prominent, all of which significantly influence CO<sub>2</sub> adsorption (Lim et al. 2016; Wang et al. 2025b).

Certain nitrogenous functional groups, such as pyridone and pyrrole, can interact with CO<sub>2</sub> through hydrogen bonds due to the proximity of the H atom to the N atom, while exhibiting energetic favorability as indicated by negative  $\Delta G_{\text{ads}}$  values. In terms of Lewis acid–base interactions, the N atom possesses a pair of lone electrons, making it electron-rich, a property that facilitates the adsorption of acidic CO<sub>2</sub>. Lim et al. (2016) employed density functional theory (DFT) to deeply analyze the interactions between various nitrogenous functional groups and CO<sub>2</sub>. It was found that these groups vary in their adsorption energies for CO<sub>2</sub>, owing to a range of interactions, including Lewis acid–base and hydrogen bond interactions. Specifically, the calculated adsorption energies ( $\Delta E_{\text{ads}}$ ) serve as quantitative indicators of binding stability, where more negative values correspond to stronger interactions. Furthermore, thermodynamic parameters, such as the isosteric heat of adsorption ( $Q_{\text{st}}$ , indicative of  $\Delta H_{\text{ads}}$ ), provide experimental corroboration of these mechanisms; CO<sub>2</sub> isotherms measured at multiple temperatures can be used to derive adsorption enthalpy ( $\Delta H_{\text{ads}}$ ) and free energy ( $\Delta G_{\text{ads}}$ ) via the Clausius-Clapeyron relationship or isotherm-based analyses, thereby quantitatively describing CO<sub>2</sub> affinity and interaction strength and enabling comparison of

the relative contributions from narrow micropores versus N-containing sites, elevated enthalpy values in nitrogen-doped biochars confirm the transition from weak physisorption to robust chemisorption driven by these functional groups. For the pyridone group, the hydrogen bond between the H atom of the hydroxyl group and the highly electronegative O of the pyridone group provides the strongest adsorption energy. The pyridine group has strong electronegativity and the adsorption mechanism is the Lewis acid–base reaction. For pyrrole group, it mainly interacts with CO<sub>2</sub> through hydrogen bonds. The pyridine-N-oxide group mainly interacts with CO<sub>2</sub> through hydrogen bonds, although these are weaker than those formed by pyridine. Consequently, its role in the Lewis acid–base reaction is less significant than that of pyridine. Other nitrogenous functional groups, such as amine, quaternary, and cyano, exhibit only weak Lewis acid–base interactions with CO<sub>2</sub>, resulting in a relatively small minimal adsorption effect on CO<sub>2</sub> (Dong et al. 2024). Here, the results of the theoretical study are compatible with experimental data, where previous experimental studies (Sai Bhargava Reddy et al. 2021) showed that biochar with pyridone, pyridine and pyrrole functional groups have strong interaction with CO<sub>2</sub>. In a study carried out by Yang et al. (2022) to develop chitosan derived N-doped microporous carbon for CO<sub>2</sub> capture, the major nitrogen-containing functional groups of porous carbon were determined by XPS analysis. It was found that while high carbonization temperatures favored the stability of graphitic-N, the presence of pyridinic and pyrrolic-N was crucial for performance, as these species are more CO<sub>2</sub>-philic than graphitic-N. It was discussed that in pyridinic nitrogen, the N atom is positioned just next to the -OH group, and the p orbital in -OH would form p- $\pi$  conjugation effect with the  $\pi$  bond. Hence, the N atom located in the ortho-position of -OH is surrounded by a higher electron density, and consequently, its Lewis basicity is improved. As a result, pyridone nitrogen serves as the main anchor for CO<sub>2</sub> capture. This experimental evidence corroborates that rational design targeting specific nitrogen configurations, such as pyridinic and pyrrolic forms, is essential. Therefore, it is imperative to adjust the porosity and surface chemistry of biochar to guarantee optimal selectivity and absorption of CO<sub>2</sub>.

#### 4 Development of engineered biochar

Biochar is a promising and cost-effective CO<sub>2</sub> adsorbent. However, its CO<sub>2</sub> absorption capacity is constrained by its limited microporosity and insufficient surface chemistry (Borhan et al. 2020). To enhance CO<sub>2</sub> adsorption, modification to biochar is necessary to improve its surface chemical attributes, particularly its alkalinity and the quantity of functional groups. These enhancements are vital to promote Lewis acid–base interactions and

hydrogen bonding, which are key molecular interactions. Utilizing various activators and conditions to modify the inherent characteristics and surface chemistry of biochar is essential for the development of “engineered biochar” that has enhanced CO<sub>2</sub> adsorption capacity and selectivity.

Engineered biochar is the modified biochar that has enhanced CO<sub>2</sub> adsorption capacity in comparison to its unmodified counterpart. It must exhibit suitable physical and chemical attributes for effective CO<sub>2</sub> adsorption (Dissanayake et al. 2020), including structural characteristics such as a large surface area and high micropore volume. These features notably augment the capacity for CO<sub>2</sub> adsorption via physical adsorption (Guo et al. 2023; Yuan et al. 2024).

To achieve the desired properties, biomass feedstock requires treatment either before or after carbonization. The production of engineered biochar necessitates a balance between structural characteristics, such as surface area and micropore volume, and surface chemical properties including alkalinity, functional groups, and hydrophobicity. This balance is key to maximizing the synergistic impact of physical and chemical adsorption (Haider et al. 2024). Specifically, this synergy becomes evident under varying conditions: at lower temperatures (e.g., 0–25 °C), physical adsorption driven by micropore filling typically dominates, contributing to high total uptake. Conversely, under elevated temperatures (typical of flue gas) or low CO<sub>2</sub> partial pressures, physical adsorption weakens. In these scenarios, chemisorption becomes paramount for maintaining capture efficiency. This chemical mechanism is primarily driven by enhanced surface basicity and active sites introduced via heteroatom doping. Subsequent sections will delve into various modification techniques, encompassing physical activation methods such as CO<sub>2</sub> and steam activation, and chemical activation approaches including amine modification and element doping. Additionally, their effects on the physicochemical properties of biochar will be explored.

#### 4.1 Physical adsorption

The physical treatment of biochar typically involves heat treatment in an activated atmosphere or with oxidizing agents to improve its pore structure, increase microporosity and mesoporosity, increase surface area, and introduce oxygen-containing functional groups. Techniques such as gas activation, ball milling, and radiation modification are commonly employed, with steam and CO<sub>2</sub> being the predominant oxidants (Igalavithana et al. 2020). At temperatures above 700 °C, these oxidants penetrate the biochar, prompting carbon atoms to vaporize. The elevated activation temperature results in the elimination of volatile substances, leading to the

creation of a highly porous biochar structure. CO<sub>2</sub> oxidation facilitates the formation and expansion of existing micropores, whereas steam activation generates both micropores and mesopores (Sajjadi et al. 2019). The selection of oxidants is key to creating microporous biochar. CO<sub>2</sub> oxidation serves to widen micropores, whereas steam activation results in the creation of both micropores and mesopores. These processes can be proceeded either during or following pyrolysis. In comparison to chemical treatments, steam or CO<sub>2</sub> activation is more industrially viable, as it eliminates the need for chemicals, reduces costs, prevents secondary pollution, saves time, and results in fewer impurities (Rashidi and Yusup 2020). Table 4 provides a review of studies on improving biochar’s CO<sub>2</sub> adsorption via physical modification.

##### 4.1.1 Activation of biochar using carbon dioxide

Gas activation predominantly utilizes oxidizing gases such as water vapor and CO<sub>2</sub>, as well as inert gases like N<sub>2</sub> and He. The gas purging process facilitates the thermal cracking of carbonaceous materials, thereby augmenting the aromatic content in biochar. This results in a decrease in its polarity and an enhancement in its hydrophobicity, thereby restricting H<sub>2</sub>O adsorption. Steam and CO<sub>2</sub> modification stand as the main gas activation techniques for biochar employed in CO<sub>2</sub> adsorption. Both techniques promote pore formation through reactions on the carbon surface of biochar. The reaction mechanism is depicted in Fig. 6a, and the comprehensive CO<sub>2</sub> activation process is delineated as follows:



Contrary to steam activation, which yields a pore distribution of micropores and mesopores, CO<sub>2</sub> activation typically generates micropores that are essential for the adsorption of small molecules such as CO<sub>2</sub>. The creation of a highly microporous biochar through CO<sub>2</sub> activation is beneficial for CO<sub>2</sub> adsorption under environmental conditions. CO<sub>2</sub> can serve as an activator during the pyrolysis of biomass feedstock (direct activation) or in post-pyrolysis treatment. The Boudouard reaction provides insight into the process of biochar activation by CO<sub>2</sub>. In this reaction, the vacant active site C<sub>f</sub> on the carbon surface adsorbs CO<sub>2</sub> through dissociative chemisorption, generating C(O) and CO (Eq. (1)). Subsequently, the C(O) on the carbon surface dissociates to CO (Eq. (2)). As the surface C(O)

**Table 4** A comprehensive summary of prior research on the physical alteration of biochar for CO<sub>2</sub> capture

Feedstock	Biochar production condition	Physical activation condition	Adsorption system	BET surface area (m <sup>2</sup> /g)	Total pore volume (cm <sup>3</sup> /g)	Micropore volume (cm <sup>3</sup> /g)	Adsorption temperature and pressure	CO <sub>2</sub> adsorption capacity (mmol/g)	Ref.
Almond shell	Pyrolyzed at 600 °C	CO <sub>2</sub> at 750 °C for 2 h	TGA	1090	0.50	n.a	25, 1 bar	2.7	(Plaza et al. 2010)
Olive stone	Pyrolyzed at 873 °C	CO <sub>2</sub> at 800 °C for 2 h	Fixed bed	909	n.a	n.a	30, 1.3 bar	9.7	(Plaza et al. 2011)
Almond shell	Pyrolyzed at 873 °C	CO <sub>2</sub> at 700 °C for 2 h	Fixed bed	831	n.a	n.a	30, 1.3 bar	13.7	(Plaza et al. 2011)
Olive stone	Direct activation	CO <sub>2</sub> at 800 °C	TGA	1215	0.51	0.48	25, 1 bar	3.1	(González et al. 2013)
Almond shell	Direct activation	CO <sub>2</sub> at 750 °C	TGA	862	0.36	0.33	25, 1 bar	2.7	(González et al. 2013)
Cotton stalk	Pyrolyzed at 600 °C	CO <sub>2</sub> at 800 °C	Fixed bed with TGA	n.a	n.a	0.24	20, 1 bar	~2.27	(Xiong et al. 2013)
Whitewood	Pyrolyzed at 500 °C	CO <sub>2</sub> at 890 °C for 100 min	Fixed bed	820	0.45	n.a	25, 1 bar	1.43	(Shahkarami et al. 2015)
Soybean straw	Pyrolyzed at 500 °C	CO <sub>2</sub> at 800 °C for 30 min	Fixed bed	346	n.a	0.19	30, 1 bar	~1.7	(Zhang et al. 2016)
Whitewood	Pyrolyzed at 500 °C	Steam activation at 700 °C for 1 h	Fixed bed	840	0.55	n.a	25, 1 bar	1.34	(Shahkarami et al. 2015)
P. nigra wood	Direct activation	Slow pyrolysis using steam at 700 °C	Surface area analyzer	217	n.a	0.093	25, 1 bar	1.12	(Gargiulo et al. 2018)
Cellulose fiber	Direct activation	Slow pyrolysis using steam at 600 °C	Surface area analyzer	593	n.a	0.220	25, 1 bar	2.33	(Gargiulo et al. 2018)
Date seed	Pyrolyzed at 800 °C	CO <sub>2</sub> at 900 °C for 1 h	Micro reaction calorimeter	798	n.a	0.28	20, 1 bar	3.21	(Ogungbenro et al. 2018)
Vine shoot	Pyrolyzed at 600 °C	CO <sub>2</sub> at 800 °C for 1 h	Surface area analyzer	767	0.374	0.245	25, 0.15 bar	1.58	(Manyà et al. 2018)
Palm kernel Shell	Direct activation	CO <sub>2</sub> at 950 °C for 60–120 min	Static volumetric instrument	508	0.364	0.233	25, 1 bar	2.5	(Rashidi and Yusup 2020)
Whitewood	Direct activation	Steam at 700 °C for 1.4 h	Single adsorption column	655	0.550	n.a	25, 1 bar	1.34	(Ghanbari and Kamath 2019)
Whitewood	Direct activation	CO <sub>2</sub> at 700 °C for 100 min	Single adsorption column	665	0.450	n.a	25, 1 bar	1.43	(Ghanbari and Kamath 2019)
Polyurethane Waste	Pyrolyzed at 400 °C	CO <sub>2</sub> at 900 °C for 2 h	Surface area analyzer	206	0.10	0.08	0, 1 bar	3.4	(Ge et al. 2019)
Pine sawdust	Pyrolyzed at 550 °C	CO <sub>2</sub> activation at 550 °C for 1 h	Surface area analyzer	581	0.25	n.a	25, n.a	0.73	(Igalavithana et al. 2020)
Olive mill	Hydrothermal carbonization at 350 °C	CO <sub>2</sub> at 850 °C for 1 h	Surface area analyzer	1135	0.476	0.373	0, 1 bar	2.95	(González and Manyà 2020)
Vine shoot	Pyrolyzed at 600 °C	CO <sub>2</sub> at 800 °C for 1 h	Surface area analyzer	536	n.a	0.161	25, 1 bar	2.67	(Manyà et al. 2020)
Wheat straw pellet	Pyrolyzed at 500 °C	CO <sub>2</sub> at 800 °C for 1 h	Surface area analyzer	514	n.a	0.191	25, 1 bar	2.44	(Manyà et al. 2020)

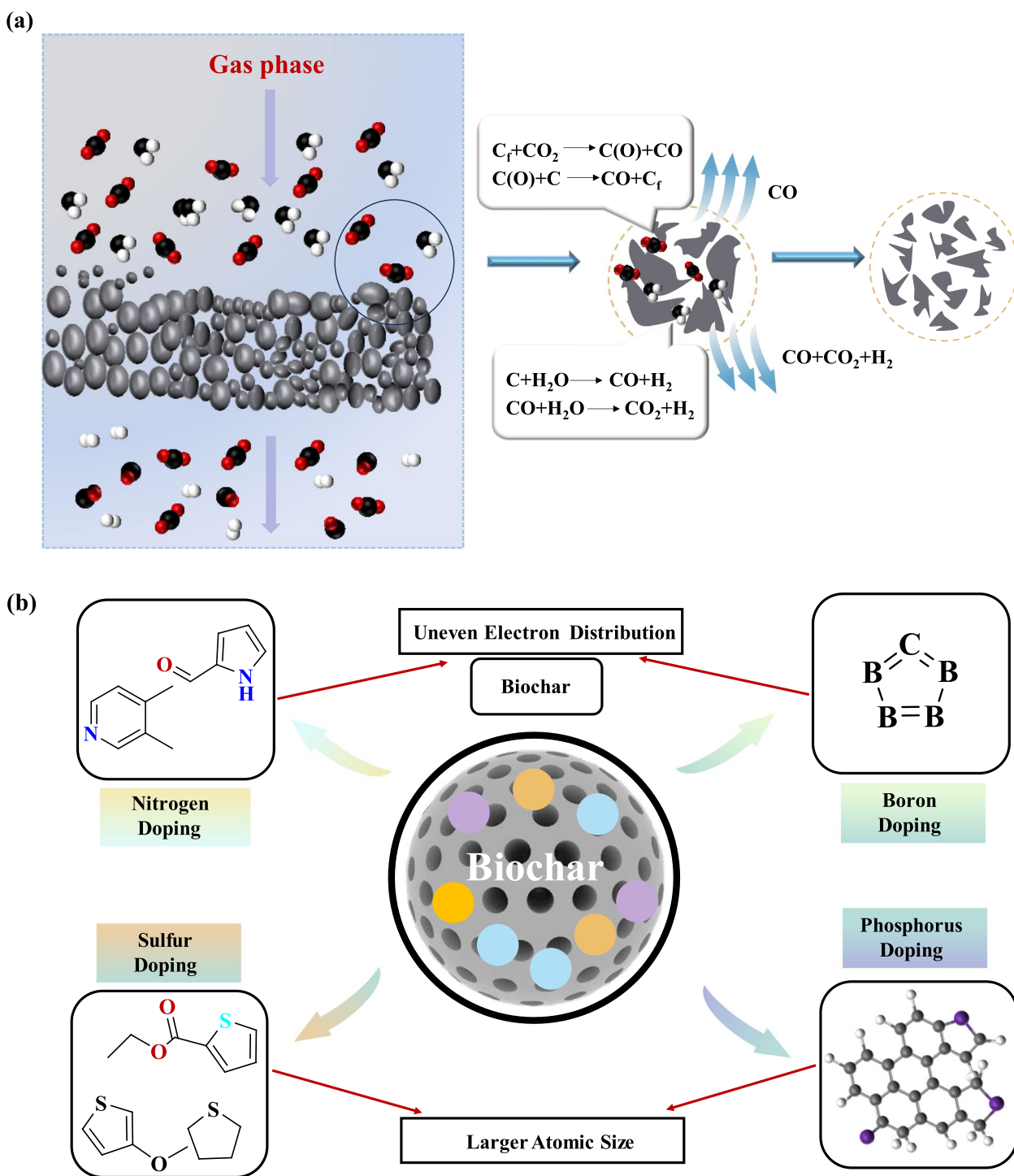


**Fig. 6** **a** Mechanism of activation using gas, and **b** the influence of four kinds of heteroatom doping on biochar. Adapted from Sun et al. (2024). Copyright 2023 Springer

complex dissociate into CO, carbon atoms are progressively removed from the lattice, leading to the development of pores. Finally, the CO present in the gaseous

product is adsorbed onto the activated carbon site, thereby inhibiting gasification (Eq. (3)).

Zhang et al. (2025c) proposed that in this reaction, CO<sub>2</sub> initially chemisorbs onto the free carbon active site (C<sub>f</sub>),

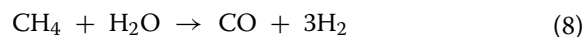
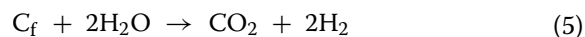
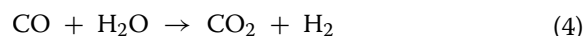
subsequently decomposing on the surface to form active carbon–oxygen complexes (C(O)) and CO. The active surface oxide then transitions from the solid phase to the gas phase, extracting one carbon atom from the carbon and generating a new vacant active site for subsequent CO<sub>2</sub> dissociative chemisorption. Ogungbenro et al. (2018) demonstrated that CO<sub>2</sub> activation of date seed carbonized at 900 °C for 1 h increased the CO<sub>2</sub> adsorption capacity of the modified biochar to 3.21 mmol/g (20 °C, 1 bar), significantly improving CO<sub>2</sub> adsorption. High CO<sub>2</sub> activation temperatures bolster micropore formation by increasing thermal corrosion and removing more carbon atoms. Consequently, when CO<sub>2</sub> activation temperatures increase, there is a corresponding increase in burnout, resulting in the removal of a larger quantity of carbon atoms. The Boudouard reaction is distinguished by a substantial positive enthalpy, approximately 172 kJ/mol at 25 °C. As a result, in order to tilt the reaction equilibrium towards the production of CO, it is necessary to employ very high temperatures that surpass 700 °C.

The parameters for CO<sub>2</sub> activation include activation temperature, CO<sub>2</sub> flow rate and holding time. Among these, temperature plays a key role in determining the structural properties of biochar. Zhang et al. (2016) observed that increasing the pyrolysis temperature, particularly up to 950 °C, augments both the surface area and pore volume of biochar. Elevated temperatures promote the endothermic reaction between CO<sub>2</sub> and the carbon matrix, thereby enhancing porosity and expanding micropores. Lower temperatures inhibit this reaction, thereby restricting porosity development. Higher activation temperatures generally enhance surface area and porosity of biochar (Abubakar et al. 2024; Kwon and Lee 2025). However, when the reaction rate surpasses the diffusion rate, the formation of micropores is constrained. Additionally, elevated temperatures can diminish surface functional groups, hydrophobicity, and biochar yield, rendering them unsuitable for industrial applications. Thus, it is imperative to strike a balance between surface area and other properties such as yield and functional groups to optimize the structure and surface chemistry of biochar.

#### 4.1.2 Activation of biochar using steam

By steam activation of biochar, porous structures are formed, and oxygen-containing functional groups such as carbonyl, ether, carboxyl, hydroxyl, and phenol groups are introduced to the carbon surface (Petrovic et al. 2021). This process can be carried out in superheated steam at 700–900 °C, with a minimum activation time of 30 min—a duration notably shorter than that required for CO<sub>2</sub> activation. The steam flow rate ranges from 120 to 300 mL/min. The smaller size of the H<sub>2</sub>O molecule allows

it to penetrate the porous carbon network more rapidly. Steam activation, akin to CO<sub>2</sub> activation, can be carried out either by directly activating the biomass or by activating after biochar pyrolysis. Theoretically, the porous structure of biochar can be enhanced by devolatilizing residual products such as ketones, aldehydes and certain acids, which are the byproducts of incomplete combustion during pyrolysis. The formation of pores during steam activation correlates with carbon depletion and the water–gas conversion reaction. As a result, steam activation can produce a wide range of pore sizes, leading to the formation of micropores and mesopores (Amer et al. 2024b; Salimi et al. 2024; Schroeder et al. 2024). The relevant reactions involved in steam activation are depicted in Eqs. (4, 5, 6, 7 and 8).



During steam activation, the oxygen in H<sub>2</sub>O interacts with active centers on the carbon surface, leading to the formation of surface oxides such as CO and hydrogen complexes (C(H)). The CO<sub>2</sub> and H<sub>2</sub> produced from the water vapor conversion reaction further stimulate surface activation, facilitating pore formation. Superheated steam simultaneously purges the trapped products from biomass pyrolysis within the pores, thereby enhancing porosity. In contrast to CO<sub>2</sub> activation, steam activation results in a wider range of pore sizes (Fig. 6a), generating both micropores and mesopores (Salimi et al. 2024; Schroeder et al. 2024).

The activation temperature significantly influences the surface area and pore volume (Razzak 2024). Below 750 °C, steam activation promotes the formation of micropores, whereas temperatures exceeding 750 °C result in a distribution of pores that includes both micropores and mesopores (Razzak 2024). Research indicates that biochar derived from barley straw, activated at 700 °C, possesses the maximum micropore surface area (540 m<sup>2</sup>/g). Elevated activation temperatures, up to 850 °C, result in the expansion of pores and the transformation of some micropores into mesopores. Nevertheless, extended activation (beyond 45 min) can lead to over-widening of the pores, thereby decreasing pore volume and surface area (Dong et al.

2025; Mochizuki et al. 2025). Consequently, determining the optimal activation temperature and duration is vital for optimizing microporosity and enhancing CO<sub>2</sub> adsorption.

#### 4.2 Chemical treatment

The chemical modification of biochar involves changing its surface structure, enhancing the micropore structure, increasing the surface area, and improving CO<sub>2</sub> adsorption capacity by introducing functional groups. This can be achieved through various methods such as alkali modification, amino modification, and metal immersion. Additionally, heteroatom doping has the potential to enrich functional groups and adjust the carbon framework, generating considerable interest due to its potential to enhance biochar properties.

Chemical adsorption typically results from the synergistic interactions among various functional groups (Xu et al. 2020; Zubbri et al. 2020), primarily hydrogen bonds and Lewis acid–base interactions involving nitrogen and sulfur functional groups. These interactions depend on the biochar's physical structure and surface chemistry. Given the Lewis acidity of CO<sub>2</sub>, functional group acting as Lewis bases can react with CO<sub>2</sub> molecules. Among chemisorption processes, those initiated by acid–base reactions are the most robust. Nitrogenous groups, such as pyridine, pyrrole, and graphite nitrogen, significantly enhance CO<sub>2</sub> adsorption capacity. Notably, 1 mol of CO<sub>2</sub> can interact with either 1 mol of pyridine nitrogen or 2 mol of pyrrole nitrogen (Mukhtar et al. 2020; Wang et al. 2020b). Amine reagents such as TETA, EDA, and TEPA are commonly used to modify biochar, leading to the formation of primary, secondary and tertiary amines on its surface. Gao et al. (2025) demonstrated that sulfur-containing functional groups and phenolic hydroxyl groups also contribute to CO<sub>2</sub> interactions, further enhancing CO<sub>2</sub> uptake. A high oxygen-to-carbon ratio in carbon materials enhances this interaction through hydrogen bonding with CO<sub>2</sub>.

In summary, CO<sub>2</sub> capture by biochar is contributed by physisorption and chemisorption. The enhancement of chemical adsorption through heteroatom doping and the improvement of physical adsorption dominance are the key factors for the design of biochar structure. The increase of micropores, specific surface area and effective functional groups are the main control factors for enhancing the adsorption capacity of biochar. As the main investigated elements for doping, nitrogen, boron, sulfur and phosphorus are used to illustrate the effects of the four dopants on biochar in Fig. 6b.

##### 4.2.1 Nitrogen doping

Among various hybrid elements, including N (Liu et al. 2021), B (Sui et al. 2021), S (Ding et al. 2020), P (Suo et al. 2019), and O (Liu et al. 2019a), N is particularly effective in doping carbon due to its proximity to carbon in the periodic table and similar atomic radii. As a result, the bond length between carbon and nitrogen closely mirrors that of carbon–carbon. This similarity facilitates the substitution of carbon atoms with nitrogenous functional groups. The incorporation of the more electronegative nitrogen atom generates a dipole moment, thereby enhancing the interaction between the positively charged carbon and external materials. This in turn augments the polarity, alkalinity, and surface activity of the biochar. Therefore, nitrogen-doped biochar (NBC) not only boasts a highly porous structure, large specific surface area, and strong intermolecular forces, but also displays significant surface activity and electrochemical properties. These include a robust ion exchange capacity, pH buffering capacity, and adsorption ability. This wide range of properties gives it broad application potential in fields such as soil treatment (Fakhar et al. 2025), CO<sub>2</sub> adsorption (Wang et al. 2021), sewage treatment (Liang et al. 2020), electrochemical energy storage (Zhou et al. 2021), and catalysis (Zhang et al. 2021).

The type of nitrogen precursor and biomass results in varying nitrogen-containing functional groups. For instance, urea phosphate promotes pore formation and amplifies surface alkalinity by generating nitrogen-containing free radicals. These free radicals form nitrogen-containing functional groups, such as pyrrole, which facilitate the degradation of the carbon surface and subsequently induce the generation of novel pores. During pyrolysis, ammonia interacts with nitrogen precursors to release free radicals that subsequently form nitrogen-containing groups on the carbon matrix, contributing to pore formation (Dong et al. 2024).

Research has demonstrated that NBC possesses a superior CO<sub>2</sub> adsorption capacity compared to original biochar. This is attributed to exceptional adsorption properties such as a high absorption rate, robust adsorption selectivity, swift adsorption kinetics, suitable adsorption heat, and high chemical and mechanical stability (Zhang et al. 2025b). The production of NBC with narrow micropores, specific nitrogen existence state, and high nitrogen content typically involves activation and in situ pyrolysis techniques. For instance, Wang et al. (2021) synthesized NBC using cyanobacteria as both carbon and nitrogen sources, coupled with KOH activation and high-temperature pyrolysis. The resultant NBC had a pore size predominantly between 0 to 2 nm and an N-Q content of 32.9%. Density functional theory (DFT) calculations (Fig. 7) showed that the electrostatic

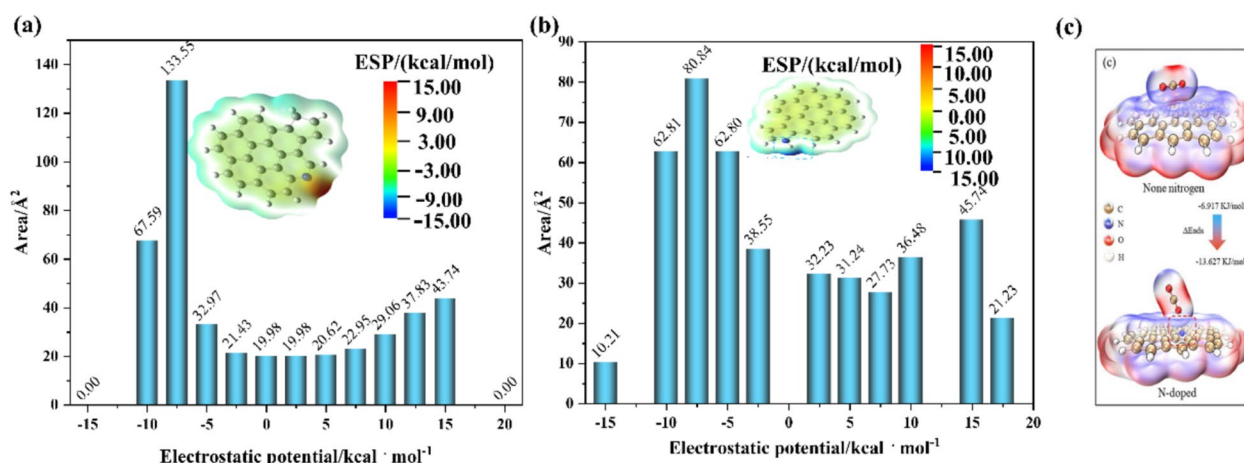


**Fig. 7** **a** Carbon skeleton of undoped graphite N atom, and **b** carbon skeleton doped with graphite N atom; **c** carbon framework with CO<sub>2</sub> being adsorbed before and after graphitic N atom doped. Adapted from Wang et al. (2021). Copyright 2021 Elsevier

potential (ESP) of the carbon skeleton in non-doped biochar was uniformly distributed (Fig. 7a). In contrast, the N-doped biochar exhibited a heterogeneous ESP distribution (Fig. 7b), with positive potential migration predominantly observed around the N-Q atoms, leading to the formation of Lewis acid/base centers. This effect augmented the CO<sub>2</sub> adsorption energy ( $\Delta E_{\text{ads}}$ ) of NBC, rendering it approximately double that of its undoped biochar (Fig. 7c). Notably, the material achieved a CO<sub>2</sub> adsorption capacity of 4.88 mmol/g at 1 bar and 0 °C, a CO<sub>2</sub>/N<sub>2</sub> selectivity ratio of 39.3%, and exhibited merely a 7% degradation after seven cycles of adsorption/desorption. This underscores its impressive separation efficiency, adsorption efficacy, and durability. The selectivity of NBC is paramount for CO<sub>2</sub> adsorption, as it effectively separates and adsorbs mixed gases, thereby enhancing collection and reutilization.

During the production of N-doped biochar, treatment temperatures that reach up to 900 °C can convert some nitrogenous groups into N-containing aromatic species. This process reduces the nitrogenous functional groups and the surface alkalinity of biochar, thereby diminishing its interaction with CO<sub>2</sub>. The modification of -COOH rich biochar using ammonium hydroxide introduces nitrile and amine groups. These N-functional groups, such as pyridinyl, pyrrole, and amide, enhance the surface basicity and polarity of biochar, thus improving its CO<sub>2</sub> adsorption capacity (Fig. 8a; Tiyawate et al. 2024). Figure 8b illustrates the reaction mechanism by which polyvinylimidazole, NH<sub>3</sub>, and HNO<sub>3</sub> interact with the native functional groups on the biochar surface, incorporating N-containing functional groups. Surface amination, typically achieved using amines like MEA, DEA, PZ, PEI, and TEPA, is a common method for introducing amino groups. Among the single amines,

TEPA exhibits a CO<sub>2</sub> adsorption capacity of 2.04 mmol/g, surpassing that of unmodified biochar (0.30 mmol/g). Cano et al. (2025) proposed a tri-stage process for the functionalization of biochar with TEPA (Fig. 9): initially, EDC activates the -COOH groups to form O-acylhydrazide as an intermediate, which then undergoes a nucleophilic reaction with amino groups to form amides and by-products such as isocyanate. Subsequently, appropriate additives (e.g., HOBt) are selected to inhibit the formation of these by-products and improve product yield; ultimately, epoxy groups interact with TEPA to produce modified biochar.

Nitrogen has similar chemical properties to carbon, facilitating its doping during or after carbonization. Nitrogen exists in two forms: chemical and structural nitrogen. Chemical nitrogen, including amino and nitroso surface functional groups, augments the Brønsted-Lowry alkalinity of carbon materials (Ouyang et al. 2021; Park et al. 2019). On the other hand, compounds containing structural nitrogen, such as pyridine, pyrrole, and graphite-nitrogen, form specific chemical bonds with carbon atoms. This enhances the Lewis basicity of the carbon materials, thereby improving the interaction with CO<sub>2</sub> and promoting adsorption performance. Moreover, the electronegativity of nitrogen modifies the electron density of neighboring carbon atoms, generating positively charged regions and special active sites within the carbon structure, further enhancing adsorption performance (Li et al. 2022c; Senthilkumaran et al. 2020).

#### 4.2.2 Sulfur doping

The process of sulfur doping notably affects the structure of biochar. Sulfur appears to be an effective strategy for modifying the structure of biochar. Sulfur, with an electronegativity of 2.58, which is close to that of carbon

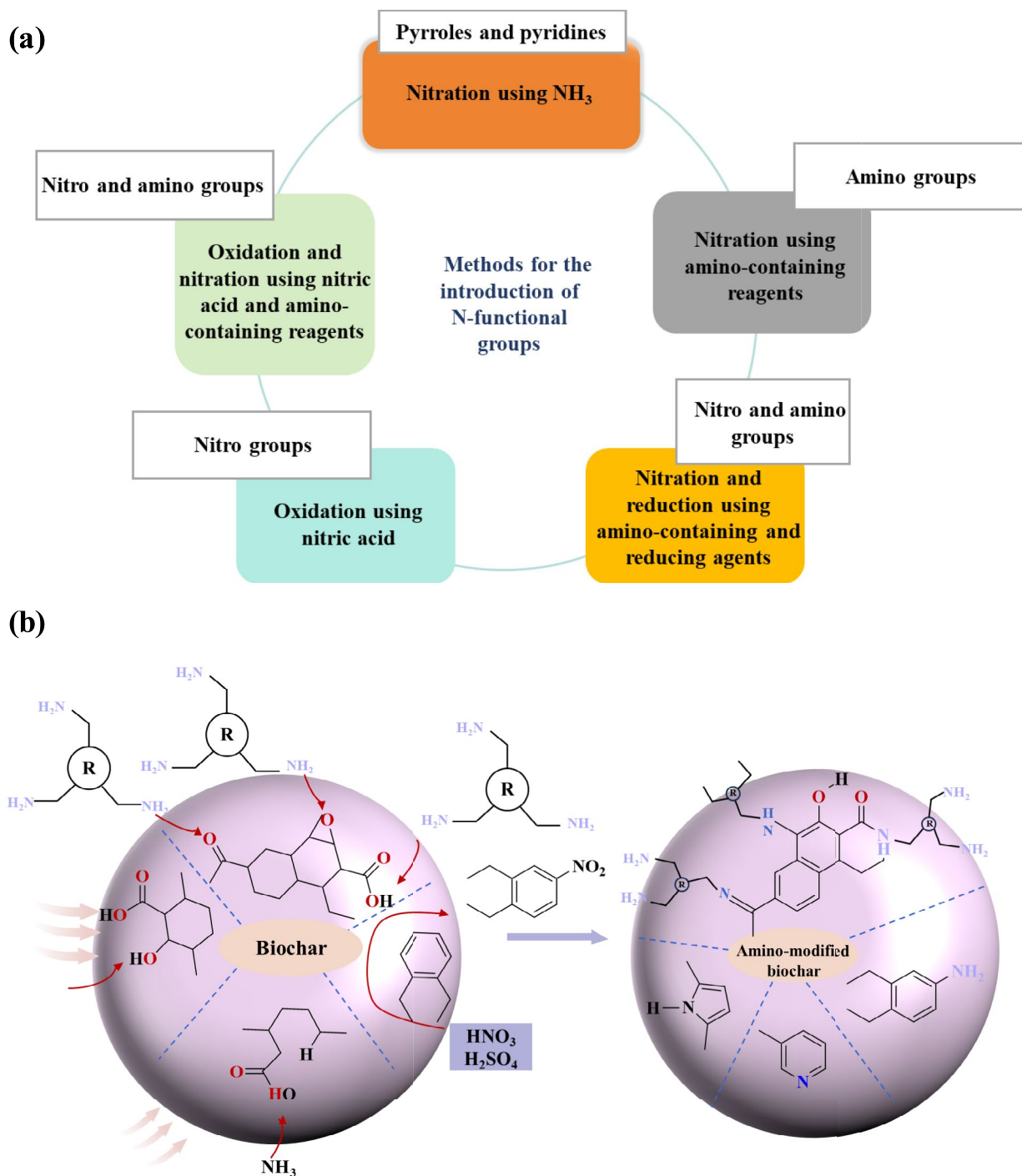


**Fig. 8** a Different nitrogenous functional groups introduced by various amination agents. Copyright 2021 Elsevier. Adapted from Shafawi et al. (2021), and b mechanism of activation using amino

(2.55), does not cause a significant imbalance in the electronegativity of doped carbon. Instead, it redistributes electrons, leading to structural defects that improve adsorption properties. This doping narrows the energy

gap between molecular orbitals, forms thiophene groups, and boosts the reactivity of catalyst, thereby improving its adsorption performance (dos Reis et al. 2024; Wang et al. 2025a). Additionally, the incorporation of sulfur

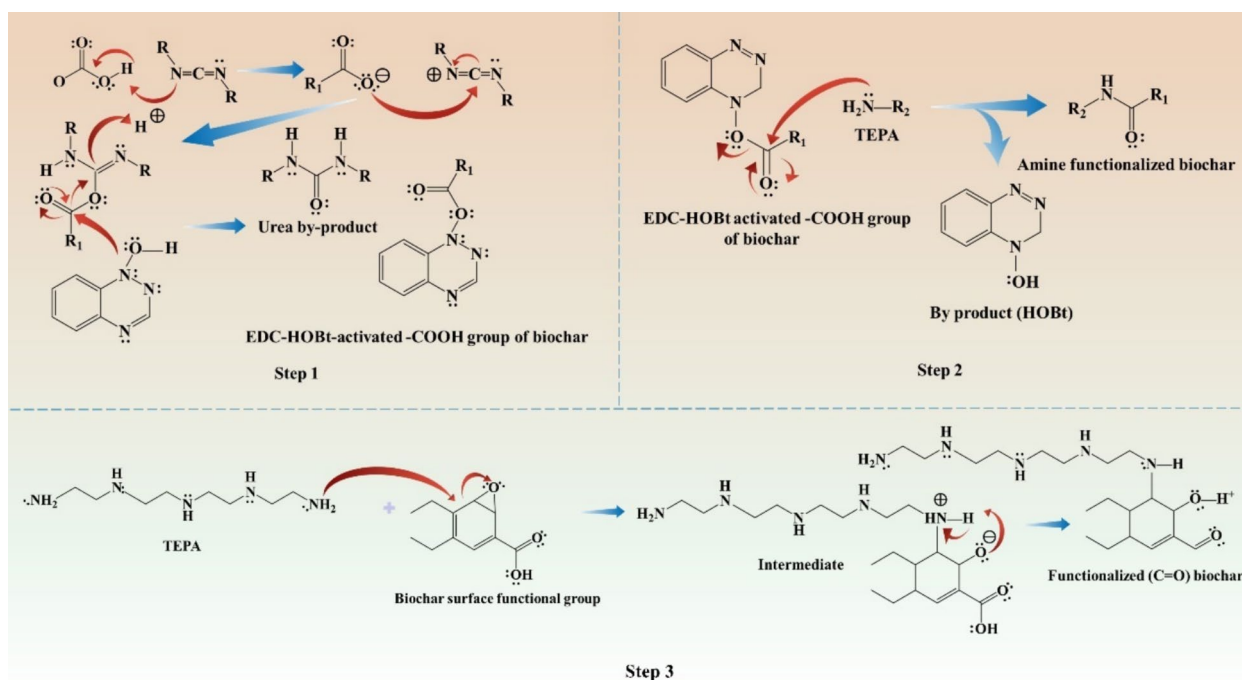


**Fig. 9** Overall mechanism of TEPA functionalization of biochar. Copyright 2018 Elsevier. Adapted from Cano et al. (2025). Step 1 represents the mechanism of EDC-HOBT coupling with the -COOH group of biochar, step 2 shows the mechanism of TEPA functionalization of the activated carbonyl group of biochar, and step 3 is the mechanism of TEPA functionalization of the activated carbonyl group of biochar

atoms can modulate the spin density and polarizability of biochar, augmenting structural defects in the carbon materials and carbon layers. Such reaction sites amplify the adsorption properties and ion storage capacity of energy storage devices. Given its abundance, cost-effectiveness, and environmental friendliness compared to transition metals, sulfur emerges as a promising dopant. The sulfur functional groups in biochar have been demonstrated to enhance the adsorption of heavy metals (Zhang et al. 2019), facilitate organic adsorption (Guo et al. 2020), enhance catalysis (Dehkhoda et al. 2010), and improve CO<sub>2</sub> capture and energy storage (Leng et al. 2019). In contrast, untreated biochar primarily relies on physical adsorption, which results in low adsorption efficiency due to the absence of active adsorption sites.

However, the presence of sulfur-containing functional groups in biochar which has been directly preserved or transformed via biomass heat treatment is relatively rare. Numerous studies have documented the loss of sulfur-containing functional groups during heat treatment, particularly at elevated temperatures. Consequently, strategies such as the selection of biomass composition, the optimization of processing parameters, and the use of additional treatments have been suggested to enhance the abundance of S functional groups in biochar (Shao et al. 2025; Yang et al. 2019). Among these approaches, the addition of sulfur during preparation stands out as

the most effective and widely employed method for introducing S functional groups, a process usually referred to as vulcanization (e.g., sulfur doping, post-treatment) (Veleghini and Pillay 2019). Vulcanization is a sophisticated chemical reaction that primarily occurs on the surface of the biochar, where unpaired electrons from unsaturated carbon atoms on the edge of the carbon plane are prone to forming bonds with the introduced sulfur atoms. The process of S doping during biochar pyrolysis or post-treatment serves as an effective vulcanization method, significantly augmenting the abundance of S functional groups.

Sulfur in biomass acts as a precursor for sulfur functional groups, which are categorized into organic sulfur (e.g., C-S, thiophene, cysteine) and inorganic sulfur (e.g., sulfates, sulfides) (Wu et al. 2019). Inorganic sulfates are absorbed by organisms, transformed into sulfides, and then combine with organic molecules to form cysteine, where sulfur exists in reduced forms such as -SH or -S-S-. This process plays a crucial role in metabolism (Bagheri Novair et al. 2024).

During the pyrolysis of biomass, certain original functional groups remain intact, while novel sulfur-based functional groups are formed through interactions with xylose present in the biomass. These groups can be categorized into volatile sulfur compounds (e.g., SO<sub>2</sub>, H<sub>2</sub>S), sulfides, and organic sulfur compounds, or alternatively

classified into reducing sulfur species (e.g., sulfides) and oxidizing sulfur species (e.g., sulfates, sulfites) (Fig. 10). For a more comprehensive classification, sulfur functional groups in biochar can be further divided into organic and inorganic categories to facilitate the study of their distinct transformation pathways (Schnieder et al. 2025) (Fig. 11).

#### 4.2.3 Phosphorus doping

Heteroatom doping, such as with P, N or S, effectively modifies carbon-based adsorbents by enhancing their chemical reactivity. When doping with heteroatoms such as N, S, and P, the physical and chemical properties of biochar are altered, endowing the material with superior performance. In particular, phosphorus-doped (P-doped) biochar exhibits enhanced adsorption performance due to phosphorus's lower electronegativity and larger covalent radius of compared to nitrogen and sulfur. This doping modifies the carbon structure and heightens polarization (Wu et al. 2022b). The introduction of heteroatoms to carbon generates defect sites, and the number of defects slightly increases with temperature. Thereby increasing the electron cloud density and material conductivity. It is observed that carbon has an electronegativity of 2.55, while phosphorus stands at 3.19. This difference suggests that carbon atoms next to phosphorus could act as Lewis base sites with lone pairs of electrons, facilitating bond formation (Liu et al. 2025). Recent research indicates that phosphorus doping in biochar can increase active sites,

thereby promoting CO<sub>2</sub> molecule adsorption on the surface of biochar. Additionally, P-doping introduces acidic sites on the carbon surface, bolstering its chemical stability as well as the adsorption of metal ions and organic compounds. The increased active sites and strong electron donor properties of P-doped biochar promote efficient CO<sub>2</sub> adsorption (Puziy et al. 2020). Research demonstrates that, among all surface functional groups, P doping markedly improves adsorption, electron acquisition, and the overall performance of materials, expanding the potential applications of activated carbon materials (Chen et al. 2021).

Studies have utilized the petioles of the aquatic plant, *Nymphaea*, as precursors to prepare biochar. The biochar is modified by phosphorus doping and KOH activating to enhance its carbon dioxide adsorption capacity (Fig. 12). Zhi's research (2025a, b, c) details the synthesis process of this innovative adsorbent, which includes pre-carbonizing the *Nymphaea* petioles at high temperatures, integrating phosphorus atoms through phytic acid modification, and ultimately activating with varying concentrations of KOH at different temperatures. The resulting adsorbent, prepared through phosphorus doping and KOH activation, reached 4.00 mmol/g at 25 °C under approximately 1 bar and 6.05 mmol/g at 0 °C (Fig. 12b). This underscores the importance of phosphorus doping in enhancing the adsorption capacity of porous carbon and provides a potential pathway for the development of high-performance CO<sub>2</sub> adsorbents using abundant biomass resources.

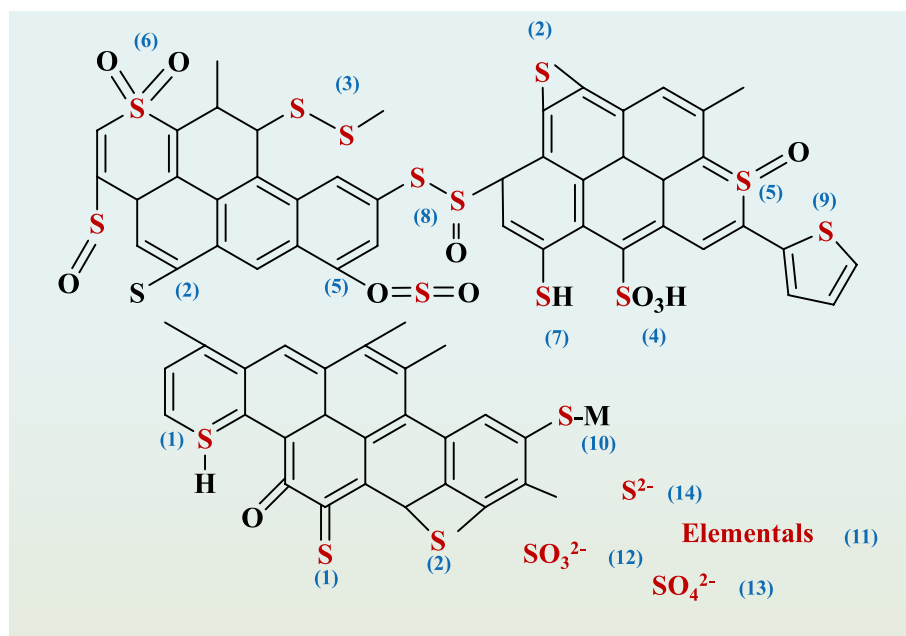


**Fig. 10** The various forms of S functionalities present on carbon surface. Adapted from Saha and Kienbaum (2019). Copyright 2019 Elsevier

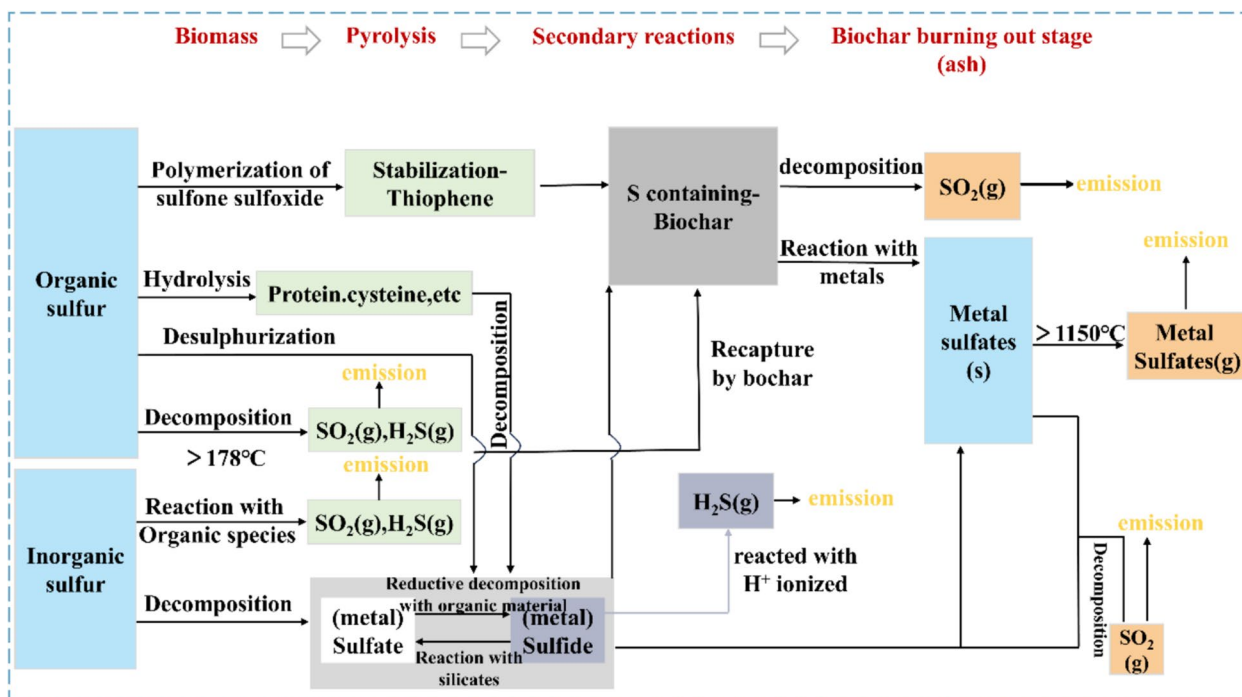


**Fig. 11** Potential reaction pathways and release mechanisms of S during biomass pyrolysis and combustion. Adapted from Liu et al. (2017) and Zhang et al. (2020). Copyright 2020 Elsevier, Copyright 2017 ACS

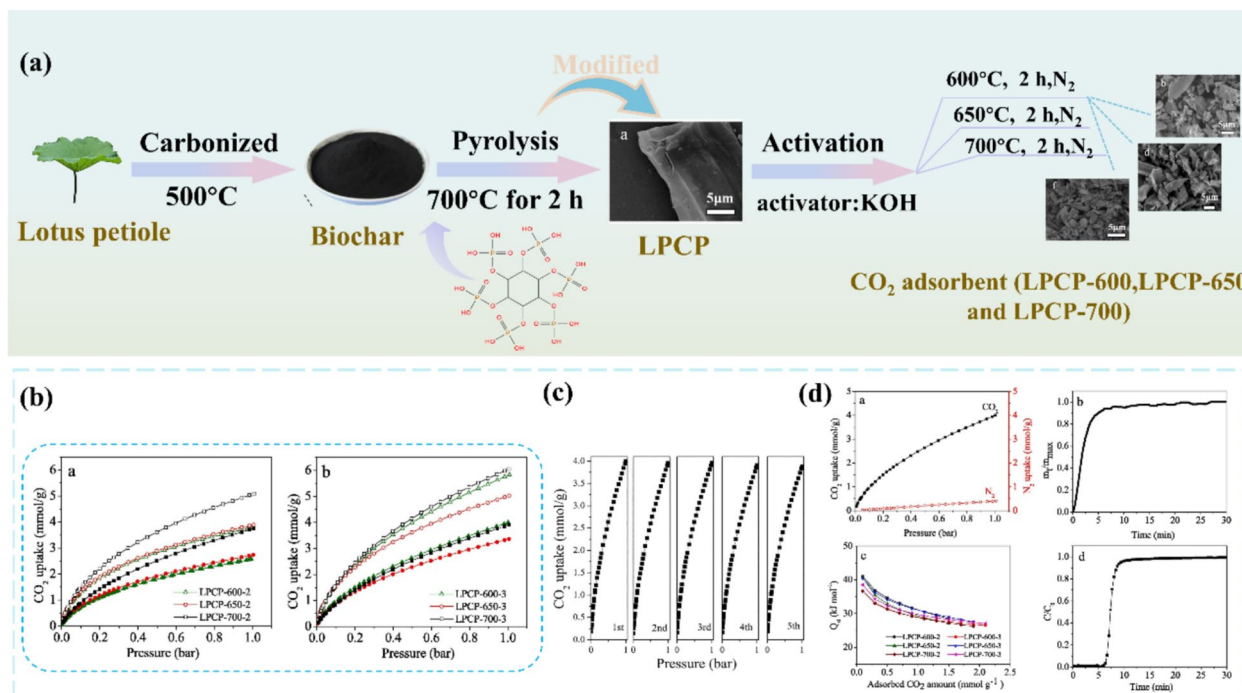


**Fig. 12 a** Steps for developing modified biochar by utilizing the petioles of lotus leaves and phosphorus doping, **b** CO<sub>2</sub> adsorption performance of various modified biochar, **c** cyclic performance of LPCP-600-3 in CO<sub>2</sub> adsorption–desorption and **d** CO<sub>2</sub> and N<sub>2</sub> isotherms of LPCP-600-3 at 25 °C and 1 bar; adsorption kinetic of CO<sub>2</sub> at 25 °C for LPCP-600-3; Q<sub>st</sub> of CO<sub>2</sub> adsorption on Lotus petiole-derived phosphorus-doped porous carbon adsorbents derived from the experimental adsorption isotherms at 0, 25 and 50 °C and breakthrough plots of LPCP-600-3 (adsorption temperature: 25 °C, gas flow rate: 10 mL/min, inlet CO<sub>2</sub> concentration: 10 vol%, gas pressure: 1 bar). Adapted from Zhi et al. (2025a). Copyright 2025 Elsevier

DFT calculations reveal that P possesses the capability to enhance porosity, making it suitable for integration with nitrogen-doped porous carbon. When P atoms are introduced, they foster the development of pyridine-N and pyrrolic-N functional groups in N-doped carbon materials. Both P and N belong to the same main group with similar chemical properties, but P has a slightly larger atomic radius than N. Notably, the C-P bond is longer than the C-N bond and exhibits a distinct polar bond orientation. This difference offers greater scope for structural modifications and variations in electron density within carbon materials. Furthermore, P predominantly exists in carbon materials as O-atom-rich  $PC_2O$ ,  $PC_2O_2$  and  $PCO_3$  functional groups, thereby enhancing the wettability of carbon materials (Ma et al. 2023). Wang et al. (2022b) found that an appropriate amount of P doping could promote the formation of defects and increase the active content in NFA-TPD-12 samples. To further improve the porosity and nitrogen content of carbon materials, nitrogen- and phosphorus-rich compounds were pyrolyzed. The effects of P groups on the pore structure of N, P-Co-doped porous carbon-X materials, N groups and the interaction between different functional groups were studied. Compared to the non-P-doped A-TDP-0 and low-P-doped A-TDP-6 materials with  $CO_2$  adsorption capacities of 4.97 and 3.01 mmol/g, respectively, the nitrogen-phosphorus co-doped material A-TDP-12 demonstrates significantly enhanced  $CO_2$  adsorption performance. With an optimized phosphorous doping concentration, it achieves capacities of 1.52 and 5.68 mmol/g at 1 and 5 bar, respectively. Moreover, its performance exhibits negligible decline after eight consecutive cycles. Thus, the strategic incorporation of phosphorus can substantially enhance the  $CO_2$  adsorption capacities of carbon materials.

#### 4.2.4 Boron doping

Research has demonstrated that the integration of heteroatomic elements can delicately adjust the electronic structure of carbon atoms, thereby generating a substantial number of active centers that can be used for catalytic reactions. Boron (B), as a neighbor of carbon in the periodic table, exhibits significant similarities with carbon at the atomic cluster scale. Consequently, it has been selected as a non-metallic element for biochar modification. The strategy of doping boron onto a carbon matrix effectively disrupts the electrical neutrality of the sp carbon-carbon network, thereby, generating new defects and charged sites for material adsorption. The atomic radius of B (1.92 Å) is smaller than that of C, with lower electronegativity (Shinde et al. 2025). Consequently, it can be incorporated into the carbon matrix, disrupting the electron-neutral two-carbon network of sp, and

inducing defects and charged sites within the adsorbent. Given these characteristics, the addition of boron can enhance the carbon material's ability to adsorb carbon dioxide. The boron-doped structure exhibits Lewis basicity, favorably interacting with the  $CO_2$  molecule, which exhibits weak Lewis acidity. Therefore, boron-doped carbon materials represent a mature choice with potential for carbon dioxide adsorption (Pan et al. 2023; Wang et al. 2025d). This process can alter the microstructure of biochar surface and optimize its activation properties, as confirmed by existing studies (Chen et al. 2025; Wang et al. 2025c). In addition, research has demonstrated that B doping can introduce B-O bonds, which serve as active sites for adsorption reactions (Pan et al. 2023). Notably, recent studies have revealed that B-doped graphene exhibits lower formation energy than N-doped graphene. B-doped tea seed shell biochar was prepared by Pan and coworkers (Pan et al. 2023). Similarly, Wang and coworkers (2025c) synthesized B-containing porous carbon derived from water chestnut shell biomass, demonstrating that boron incorporation effectively modulates the carbon framework and generates oxygen-coordinated boron species. It was found that the presence of boron-oxygen functional motifs (e.g., -O-B-O) significantly improves the adsorption performance of modified carbon materials by enhancing surface polarity and  $CO_2$  affinity. Consequently, B-doped biochar derived from sustainable biomass feedstocks is anticipated to be an ideal candidate material for achieving high  $CO_2$  adsorption capacity and stability.

#### 4.2.5 Co doping

Research (Wu et al. 2024a) has demonstrated that the multi-element co-doping of biochar is notably more effective in enhancing its performance in comparison to single-element doping. This can be attributed to the synergistic effects of multi-element co-doping and assorted functional groups, which augment the active sites on the surface of porous carbon, thereby bolstering its adsorption performance. The heterogeneous atom doping (incorporating elements such as N, O, S, P, and halogens) has been identified as a successful technique for increasing the active sites on the surface of porous carbon. This method of heterogeneous doping has the potential to generate a diverse array of functional groups that contain heteroatoms within the carbon lattice (Fig. 13a). The study conducted by Shi et al. (2022) resulted in the synthesis of N-O co-doped porous carbon using melamine-urea-formaldehyde resin as a carbon precursor. The resultant product exhibited an impressive specific surface area of 2784.53  $m^2/g$  and a superior  $CO_2$  adsorption capacity of 18.49 mmol/g at 25 °C and 1 bar. The enhancement in  $CO_2$  interactions was attributed

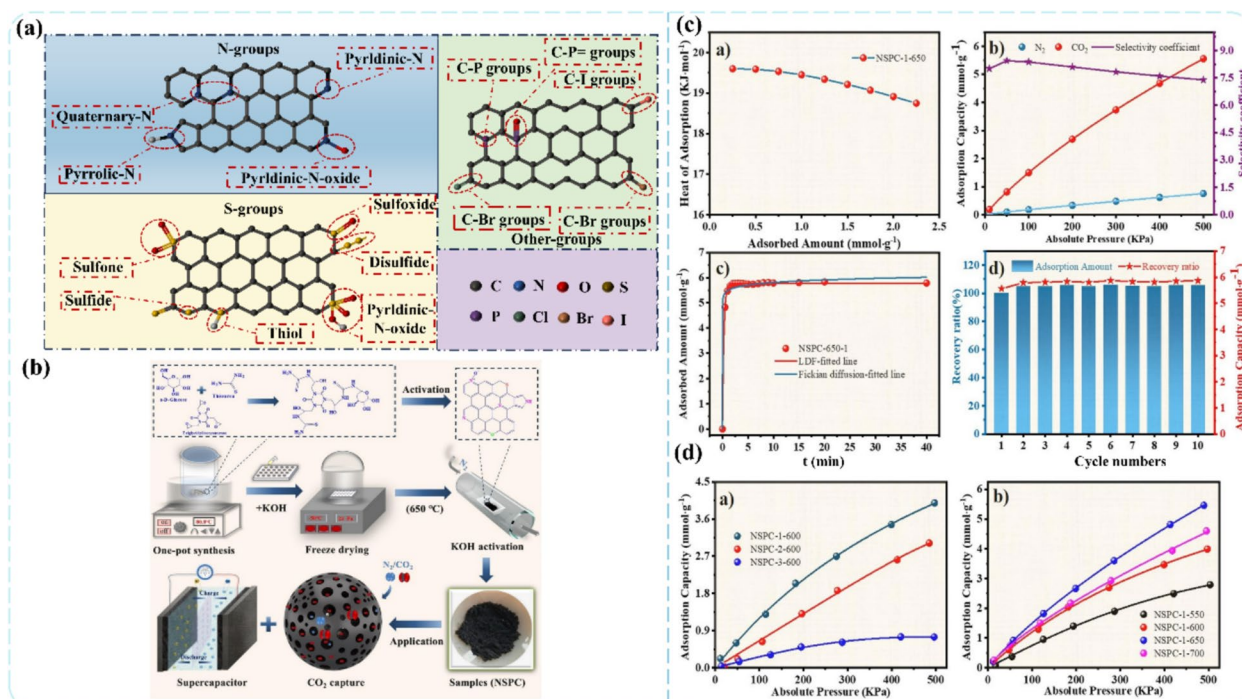


**Fig. 13** a A scheme of the of different types of heteroatom containing functional groups on porous carbon. Copyright 2024 Elsevier. Adapted from Wu et al. (2024a) b schematic illustration of the condensation of porous carbon and the synthesis and application of N,S-co-doped porous carbon material, c heat of CO<sub>2</sub> adsorption on NSPC-1-650 calculated from the experimental adsorption isotherms at 15 to 50 °C; CO<sub>2</sub> and N<sub>2</sub> adsorption isothermal curves and selectivity coefficient of NSPC-1-650 at 25 °C; CO<sub>2</sub> adsorption kinetics and curve fitting; and CO<sub>2</sub> regenerative test of NSPC-1-650 at 25 °C and 5 bar, and d isothermal adsorption curves of CO<sub>2</sub> under different activator ratios and activation temperatures at 25 °C. Adapted from Xiao et al. (2021). Copyright 2021 Elsevier

to the presence of N–O functional groups, which facilitated multilayer adsorption. A nitrogen-sulfur co-doped porous carbon was synthesized by Xiao et al. by using a single-step condensation process with trimellitic anhydride, glucose, and thiourea (Fig. 13b) (Xiao et al. 2021). This material demonstrated superior CO<sub>2</sub> absorption capacity (5.56 mmol/g), rapid adsorption kinetics, and exceptional regeneration ability (Fig. 13c, d). The co-doping of nitrogen and sulfur could significantly enhance CO<sub>2</sub> adsorption in carbon materials, with the contents of nitrogen and sulfur being critical factors (Shao et al. 2022).

Heteroatom doping modifies the surface charge distribution and augments the number of active sites, thereby enhancing CO<sub>2</sub> adsorption. Nitrogen, phosphorus, and boron create functional groups that amplify the Lewis acid–base properties of biochar. On the other hand, sulfur and phosphorus, owing to their larger atomic size, induce defects in the carbon structure, which further escalates the number of active sites. This process can broaden the pore structure of pure biochar, increasing both the surface area and the number of active sites, consequently improving its adsorption performance. For optimal doping effects, the techniques and conditions

of heteroatom doping must be meticulously examined, with pre-modification and post-modification doping constituting the two primary approaches (Xiao et al. 2021). While the choice of co-doping elements, techniques, and the underlying mechanisms of co-doping's impact on CO<sub>2</sub> adsorption are not yet fully understood (Sun et al. 2023b; Wu et al. 2024a), further research is required to elucidate the synergistic effects of various heteroatoms in augmenting CO<sub>2</sub> adsorption.

## 5 Doping method

### 5.1 Pre-doping method

The process of pre-doping, alternatively referred to as in-situ synthesis, entails the addition of N sources to raw materials prior to carbonization or the utilization of precursors containing both N and C as raw materials. This in-situ synthesis can be further categorized into various methods, including the activation method, hydrothermal method, pyrolysis method, and template method among others. The introduction of N sources during the carbonization process ensures that the nitrogen protons are distributed evenly within the carbon skeleton, resulting in a superior doping effect and high nitrogen content. The nitrogen in the prepared

carbon material primarily exists as relatively stable structural nitrogen (Mou et al. 2021). Table 5 provides a summary of the different raw materials and biochar preparation methods used for the pre-decoration of heteroatom-doped biochar. Such biochar exhibits superior CO<sub>2</sub> adsorption performance under standard pressure and room temperature. For illustrative purposes, a direct comparison with an unmodified counterpart is included for the sample from (Han et al. 2019) to demonstrate the significant enhancement afforded by the modification. For pyrolytic carbonization method, it refers to the direct pyrolysis of biomass into biochar under a limited oxygen or inert gas atmosphere (Li et al. 2022b). This method offers several advantages over others, including simplicity, convenience, a broad adjustable temperature range, and easy control. The process of nitrogen-doped pyrolysis carbonization is illustrated in Fig. 14a. However, research has shown that although nitrogen doping can enhance the CO<sub>2</sub> adsorption performance of biochar, the primary factor influencing its CO<sub>2</sub> adsorption is the physical adsorption predicated on optimal pore structure characteristics. Therefore, it is essential to employ common chemical activation methods to create an effective pore structure. However, chemical activation may alter the nitrogen structure in biochar and reduce its nitrogen content. Future research should aim to enhance CO<sub>2</sub> adsorption performance through nitrogen doping, while preserving the biochar's optimal chemical activity and pore formation, and avoiding undesirable changes in nitrogen structure and loss of nitrogen content.

## 5.2 Post-doping method

Post-doping method, also known as post-treatment method, refers to the process of preparing carbon materials and modifying biochar with N-containing compounds to produce NBC (Li et al. 2025). Typical sources of nitrogen utilized in this process include NH<sub>3</sub>, ammonium salts, nitric acid, urea, melamine, and aniline. The type of N doped via this method is primarily influenced by the reaction temperature. At lower temperatures, nitrogen predominantly exists as chemical nitrogen, resulting in minimal alterations in surface properties and pore structure. Conversely, at higher temperatures (e.g., above 700 °C), C atoms are substituted by some N atoms, manifesting as structured N within NBC. This results in a higher N content (Niu et al. 2023). Figure 14b illustrates the process flow involved in preparing nitrogen-doped biochar using the post-decoration method. Post-treatment methods, such as KOH activation, can increase N-Q content but may alter the pore structure, thereby diminishing the efficiency of CO<sub>2</sub> adsorption. Additionally, ball milling is a technique that introduces N-containing functional groups to the surface, although the quantity of N doping remains relatively low. For instance, after undergoing ball milling with ammonia, the N content in bagasse increased from 0.3% to 1.8% (Dong et al. 2024).

Compared to pre-doping method, post-modification of biochar generally exhibits lower heteroatom content and poorer CO<sub>2</sub> adsorption due to the potential instability of the heteroatomic structures. Conversely, pre-doping method incorporates heteroatoms

**Table 5** The production of heteroatom-doped biochar obtained by the method of pre-decoration doping

Biomass	Heteroatom source	Biochar preparation	Doping elements	CO <sub>2</sub> uptake (mmol/g, 25 °C and 1 bar)*	Ref.
Longan shell	Carbamide	Pyrolysis 700 °C, 2 h	N	4.30	(Wei et al. 2017)
Glucosamine Hydrochloride	Self doped	Hydrothermal 200 °C, 6 h	N	4.50	(Shi et al. 2017b)
Water chestnut shell	Sodium amide	Pyrolysis 500 °C, 2 h	N	4.50	(Rao et al. 2019)
Sugarcane bagasse	Carbamide	Pyrolysis 600 °C, 0.5 h	N	4.80	(Han et al. 2019)
Resorcinol–formaldehyde resin	H <sub>2</sub> SO <sub>4</sub>	Pyrolysis 500 °C, 2 h	S	3.69	(Shi et al. 2017a)
L-glutamic acid	thiourea	Pyrolysis 550 °C, 1 h	N, S	3.54	(Shao et al. 2022)
Cornstalks	melamine; phytic acid	Pyrolysis 400 °C, 2 h	N, P	3.10	(Yuan et al. 2022)
Sugarcane bagasse	none	Pyrolysis 600 °C, 0.5 h	none	2.32	(Han et al. 2019)

\* CO<sub>2</sub> uptake at 25 °C and 1 bar (mmol/g)

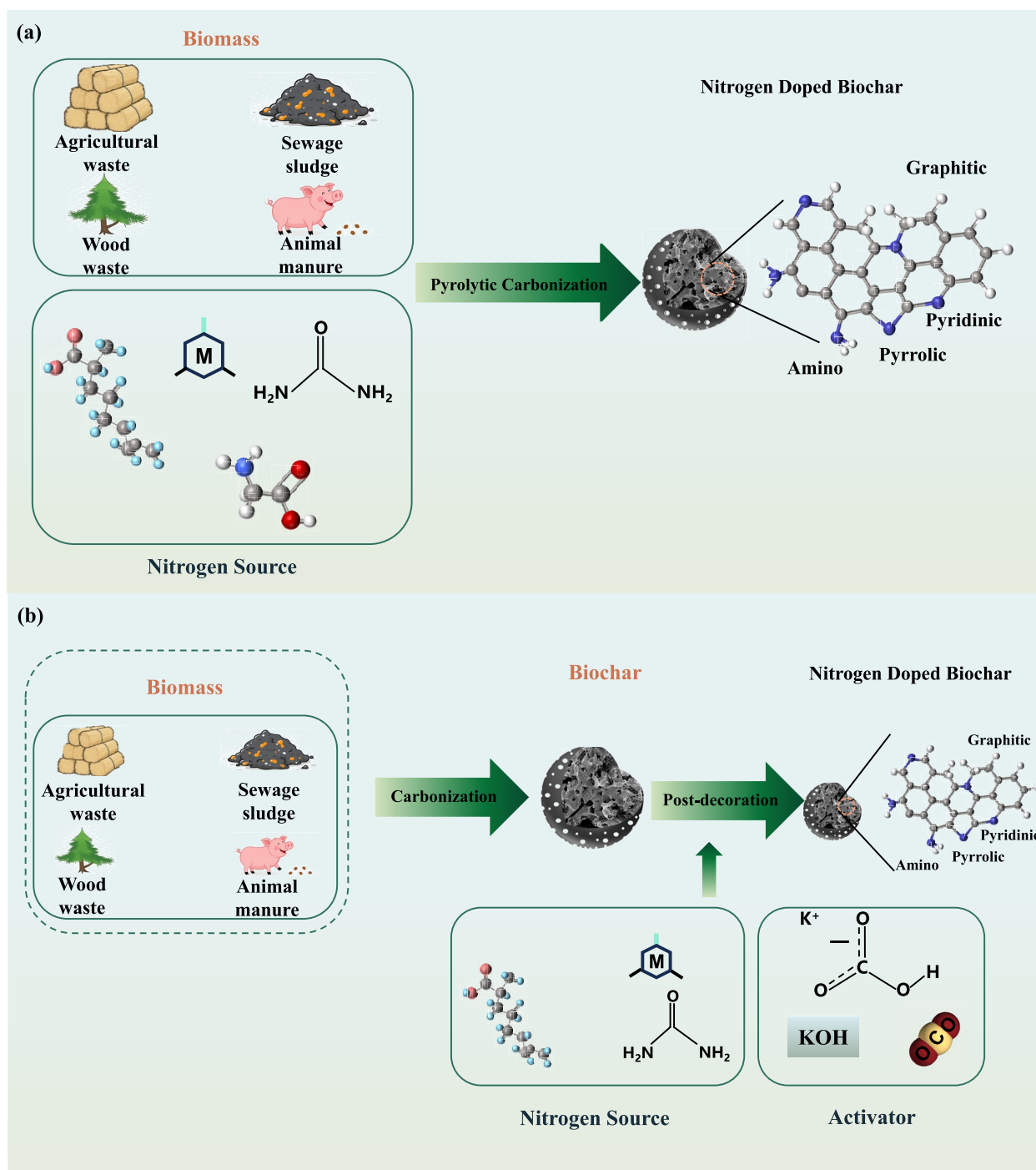


**Fig. 14** **a** Pyrolysis carbonization with nitrogen doping, and **b** process of producing nitrogen-doped biochar by post-decoration. Adapted from Sun et al. (2024). Copyright 2023 Springer

during the polymerization process of the carbon skeleton, resulting in more stable modifications. Future research should focus on improving post-modification

techniques to bolster doping efficiency, stabilize functional groups, and optimize pore structures for better performance (Sun et al. 2024).

## 6 Reusability of biochar

For economic viability and large-scale applications, it is essential to ascertain the regenerative capacity of biochar in consecutive CO<sub>2</sub> adsorption–desorption processes. Beyond its high adsorption capacity, the adsorbent must exhibit consistent performance throughout the regeneration process. The reusability of biochar is essential for CO<sub>2</sub> capture, especially in large-scale applications.

Research has demonstrated that biochar derived from wheat grass particles through CO<sub>2</sub> activation maintains stability across five adsorption–desorption cycles, exhibiting an 18.2% reduction in CO<sub>2</sub> capture capacity (Manyà et al. 2020). Biochar produced from pine sawdust via KOH-activation retains a consistent CO<sub>2</sub> adsorption capacity throughout 15 cycles (Quan et al. 2020). Meanwhile, rambutan peel biochar doped with MgO displays steady performance over 25 cycles (Zubbri et al. 2020). Similarly, Mg-loaded walnut shell biochar shows no significant CO<sub>2</sub> adsorption capacity loss after 10 cycles (Lahijani et al. 2018). Moreover, various biochars, including those sourced from pine and pecan, among others, demonstrate remarkable reusability, with all adsorbents regaining up to 90% of their initial adsorption capacity within 10 cycles (Cao et al. 2022). However, white wood steam-activated biochar experiences a decline in adsorption capacity after 20 cycles (Francis et al. 2023), suggesting that steam-activated biochar is not stable in multiple CO<sub>2</sub> adsorption–desorption cycles, and regeneration is needed.

The regeneration capacity of biochar is intrinsically linked to the isosteric heat of adsorption ( $Q_{st}$ ), a measure of the interaction strength between the adsorbent and CO<sub>2</sub>. A higher  $Q_{st}$  value corresponding to the filling of ultrafine pores, while a lower  $Q_{st}$  value suggests weaker CO<sub>2</sub> interactions within larger pores (Wang et al. 2024a). The presence of ash in biochar has the potential to block micropores and hinder physical adsorption. However, the ash contributes to the chemisorption of CO<sub>2</sub>, a process that is irreversible. Analyses indicate that the primary cause of the decline in adsorption capacity of biochar is the incomplete release of CO<sub>2</sub> molecules chemically bonded to biochar during the adsorption–desorption cycle. For heteroatom-doped biochar, such as melamine-modified rice husk biochar, which primarily depends on CO<sub>2</sub> chemisorption, elevated regeneration temperatures may be necessary for CO<sub>2</sub> desorption. However, even under these conditions, some adsorbed CO<sub>2</sub> may not be regenerated, resulting in a reduction of adsorption capacity. This observation aligns with the results reported by Li et al. (2022a), where biochar activated at higher temperatures (700–800 °C) showed slight activity loss after 10 cycles (Li et al. 2022a). Biochar was produced from a mixture of sewage sludge and pine

sawdust, and subsequently activated with KOH at various activation temperatures (600, 700 and 800 °C). After 10 cycles, the activity of biochar activated at 700 °C and 800 °C decreased by 3% and 2%, respectively.

From both technical and economic standpoints, it is imperative to have an adsorbent that possesses high CO<sub>2</sub> capture capacity and maintains stable performance across multiple cycles of adsorption–desorption. This is essential to guarantee the viability of the adsorption process.

## 7 Conclusion and Perspectives

### 7.1 Conclusion

Biochar has gained recognition as a remarkably promising material for CO<sub>2</sub> adsorption, owing to its environmentally friendly properties, cost-effective production, and adaptable physicochemical attributes. This review highlights that engineered biochar is not merely a simple carbon skeleton but serves as a highly tailorable physicochemical framework. Through heteroatom doping (N, S, P, B) and activation processes (encompassing both physical and chemical activation), it enables the synergistic optimization of surface chemistry and microporous structure. On the one hand, ultramicropores/micropores provide pore-filling and molecular sieving effects, which largely determine capacity and selectivity at low temperature and low partial pressure. On the other hand, introducing specific functional groups—particularly pyridinic and pyrrolic nitrogen—effectively bridges the gap between physical adsorption capacity and chemical selectivity. These groups modulate adsorption strength and gas selectivity through Lewis acid–base interactions, hydrogen bonding, and van der Waals forces. Consequently, this enables highly efficient CO<sub>2</sub> capture even under low partial pressures. However, bridging the chasm between laboratory breakthroughs and industrial deployment requires a pragmatic confrontation of current limitations. While modifications enhance performance, they often incur higher energy consumption and production costs. However, the transition to industrial viability faces several hurdles. Key challenges include uncertainties in techno-economic feasibility and potential performance degradation over long-term cycles. Furthermore, the lack of standardized protocols for characterizing biochar heterogeneity remains a critical barrier.

### 7.2 Overarching perspectives

To advance biochar-based adsorbents toward industrial CO<sub>2</sub> capture, future research should move beyond maximizing single-gas uptake and increasingly address manufacturability, regenerability, and process integration. Key directions include:

- (1) Condition-oriented structure-chemistry co-design: optimizing the balance among ultramicroporosity, N-functionalities, selectivity, and regenerability for targeted scenarios (post-combustion capture, gas upgrading, or DAC).
- (2) A closed loop between mechanism and identification: combining operando/quasi-operando characterization with theoretical calculations to quantitatively link pore filling, hydrogen bonding, van der Waals forces, and Lewis acid–base interactions to adsorption thermodynamics and kinetics; strengthening reproducible identification of N-species using cross-validated techniques such as XPS and FTIR to mitigate uncertainties from peak overlap.
- (3) Validation in realistic gas mixtures and cyclic operation: prioritizing tests under the coexistence of H<sub>2</sub>O, SO<sub>2</sub>, and multicomponent gases to determine competitive adsorption, selectivity retention, and performance decay, together with systematic comparisons of regeneration modes (TSA/VSA/PSA) in terms of energy demand and structural stability.
- (4) Pilot-scale scale-up and process integration: promoting pilot fixed-bed and pressure-/vacuum-swing tests, establishing traceable links among feedstock, synthesis, pore/chemistry descriptors, performance, and cycle life; and assessing compatibility with practical capture units or utilization processes.
- (5) Industrial constraints and policy coupling: extending evaluation to life-cycle considerations, feedstock logistics, and process safety (e.g., activator corrosion), and connecting material development with policy incentives and carbon-market mechanisms.

In summary, biochar shows strong promise for CO<sub>2</sub> capture, yet its role as a CCUS-enabling material must be assessed in a balanced manner against the remaining technical and economic barriers, particularly scalable manufacturing with consistent quality, long-term stability in humid/impurity streams, and demonstrably low-energy regeneration coupled with system-level integration. Interdisciplinary collaboration should therefore focus on coordinated advances across materials, processes, equipment, and policy frameworks to bridge laboratory performance to engineering validation.

#### Authors' contributions

The study concept and design were performed by Xiangping Li, Xuanxuan Li and Peng Liang. The material preparation, data collection and analysis were performed by Caixia Zhang and Yifei Yu. The first draft of the manuscript was written by Xiangping Li and Xuanxuan Li. The review and editing were conducted by Qing Liu, Mahesh Hordagoda, Wenbing Ding, Shengshu Xu, Thilini

U. Ariyadasa, P. H. V. Nimarshana and Xizhuang Qin. All authors read and approved the final manuscript.

#### Funding

This work was supported by the National Natural Science Foundation of China [grant number 22378236], Shandong Provincial Natural Science Foundation [grant number ZR2022MB108], The International Cooperation and Exchange Programme (NSFC) [grant number W2412090] and Special Project on Key Research and Development Tasks of Xinjiang Autonomous Region [grant number 2022B03029-2].

#### Data availability

The datasets used or analyzed during the current study are available from the corresponding author on reasonable requests.

#### Declarations

#### Competing interests

The authors declare that they have no known competing financial interests or personal relationships that could have appeared to influence the work reported in this paper.

#### Author details

<sup>1</sup>Shandong Key Laboratory of Coal Staged Conversion and Low Carbon Utilization, College of Chemical and Biological Engineering, Shandong University of Science and Technology, Qingdao, Shandong 266590, China. <sup>2</sup>Department of Mechanical Engineering, University of Moratuwa, Moratuwa 10400, Sri Lanka. <sup>3</sup>Department of Chemical and Process Engineering, University of Moratuwa, Moratuwa 10400, Sri Lanka.

Received: 28 September 2025 Revised: 30 January 2026 Accepted: 3 February 2026

Published online: 13 April 2026

#### References

- Abd AA, Naji SZ, Hashim AS, Othman MR (2020) Carbon dioxide removal through physical adsorption using carbonaceous and non-carbonaceous adsorbents: a review. *J Environ Chem Eng* 8(5):104142. <https://doi.org/10.1016/j.jece.2020.104142>
- Abubakar I, Saeed MD, Ayuba AM (2024) Physicochemical properties of biochar prepared from guinea corn straw as a function of different pyrolysis temperatures. *J Envi Sci Agri Res* 2(4):1–8. <https://doi.org/10.61440/jesar.2024.v2.37>
- Ahmed MB, Zhou JL, Ngo HH, Guo W, Chen M (2016) Progress in the preparation and application of modified biochar for improved contaminant removal from water and wastewater. *Bioresour Technol* 214:836–851. <https://doi.org/10.1016/j.biortech.2016.05.057>
- Ali B, Razak SA, Arshad A, Javed MA, Batool R, Hafeez A, Ali S, Khan MN, Singh N, Garhwal V, Fahad S (2025) Biochar: an overview. *Biochar for Mitigating Abiotic Stress* 1–12. <https://doi.org/10.1016/B978-0-443-24137-6.00001-X>
- Amer NM, Lahijani P, Mohammadi M, Mohamed AR (2024a) Modification of biomass-derived biochar: a practical approach towards development of sustainable CO<sub>2</sub> adsorbent. *Biomass Convers Biorefin* 14(6):7401–7448. <https://doi.org/10.1007/s13399-022-02905-3>
- Amer NM, Lahijani P, Mohammadi M, Mohamed AR, Anthonysamy SI (2024b) Woody biomass-derived biochar decorated with vanadium oxide as a potential adsorbent for CO<sub>2</sub> capture. *Int J Environ Res Public Health* 18(3):43. <https://doi.org/10.1007/s41742-024-00605-6>
- Bagheri Novair S, Biglari Z, Asgari Lajayer B, Shu W, Price GW (2024) The role of sulphate-reducing bacteria (SRB) in bioremediation of sulphate-rich wastewater: focus on the source of electron donors. *Process Saf Environ Prot* 184:190–207. <https://doi.org/10.1016/j.psep.2024.01.103>
- Beljin J, Đukanović N, Anojčić J, Simetić T, Apostolović T, Mutić S, Maletić S (2024) Biochar in the remediation of organic pollutants in water: a review of polycyclic aromatic hydrocarbon and pesticide removal. *Nanomaterials* 15(1):26. <https://doi.org/10.3390/nano15010026>

- Borhan A, Yusup S, Mun YS (2020) Surface modification of rubber seed shell activated carbon with malic acid for high CO<sub>2</sub> adsorption. IOP Conf Ser: Earth Environ Sci 460(1):012044. <https://doi.org/10.1088/1755-1315/460/1/012044>
- Cano FJ, Sánchez-Albores R, Ashok A, Escorcía-García J, Cruz-Salomón A, Reyes-Vallejo O, Sebastian PJ, Velumani S (2025) *Carica papaya* seed-derived functionalized biochar: an environmentally friendly and efficient alternative for dye adsorption. J Mater Sci Mater Electron 36(11):663. <https://doi.org/10.1007/s10854-025-14725-y>
- Cao L, Zhang X, Xu Y, Xiang W, Wang R, Ding F, Hong P, Gao B (2022) Straw and wood based biochar for CO<sub>2</sub> capture: adsorption performance and governing mechanisms. Sep Purif Technol 287:120592. <https://doi.org/10.1016/j.seppur.2022.120592>
- Chatterjee R, Sajjadi B, Chen WY, Mattern DL, Hammer N, Raman V, Dorris A (2020) Effect of pyrolysis temperature on physicochemical properties and acoustic-based amination of biochar for efficient CO<sub>2</sub> adsorption. Front Energy Res 8:85. <https://doi.org/10.3389/fenrg.2020.00085>
- Chen H, Guo Y, Du Y, Xu X, Su C, Zeng Z, Li L (2021) The synergistic effects of surface functional groups and pore sizes on CO<sub>2</sub> adsorption by GCMC and DFT simulations. Chem Eng J 415:128824. <https://doi.org/10.1016/j.cej.2021.128824>
- Chen Y, Zhang Y, Meng H, Cui J, Hayat W, Zhuo Y, Jia CQ (2025) Insight into algae-derived boron-doped biochar for efficient peroxydisulfate activation: the dominant effect of electron-transfer processes. J Environ Chem Eng 13(3):116324. <https://doi.org/10.1016/j.jece.2025.116324>
- Cui J (2022) Recent advances in post-combustion CO<sub>2</sub> capture via adsorption methods. Highlights in Science, Engineering and Technology 6:172–181. <https://doi.org/10.54097/hset.v6i.959>
- Dai Y, Zhang N, Xing C, Cui Q, Sun Q (2019) The adsorption, regeneration and engineering applications of biochar for removal organic pollutants: a review. Chemosphere 223:12–27. <https://doi.org/10.1016/j.chemosphere.2019.01.161>
- Dekhkhoda AM, West AH, Ellis N (2010) Biochar based solid acid catalyst for biodiesel production. Appl Catal A Gen 382(2):197–204. <https://doi.org/10.1016/j.apcata.2010.04.051>
- Ding D, Yang S, Qian X, Chen L, Cai T (2020) Nitrogen-doping positively whilst sulfur-doping negatively affect the catalytic activity of biochar for the degradation of organic contaminant. Appl Catal B Environ 263:118348. <https://doi.org/10.1016/j.apcatb.2019.118348>
- Dissanayake PD, You S, Igalavithana AD, Xia Y, Bhatnagar A, Gupta S, Kua HW, Kim S, Kwon JH, Tsang DCW, Ok YS (2020) Biochar-based adsorbents for carbon dioxide capture: a critical review. Renew Sust Energy Rev 119:109582. <https://doi.org/10.1016/j.rser.2019.109582>
- Dong J, Wang R, Wang X, Tan S, Zhao Z, Yin Q, Lu X (2024) Preparation of lignin-based porous carbon through thermochemical activation and nitrogen doping for CO<sub>2</sub> selective adsorption. Carbon 229:119530. <https://doi.org/10.1016/j.carbon.2024.119530>
- Dong J, Wang R, Xie Y, Gao F, Tan S, Zhao Z, Yin Q, Hu EJ (2025) Interpretable machine learning analysis on CO<sub>2</sub> adsorption and separation capacity of biochar under multi-scenario conditions. Green Energy Environ. <https://doi.org/10.1016/j.gee.2025.07.001>
- Donger E, Bhatia A, Pegram J, Kelly O (2025) Inclusion of children and youth in the intergovernmental panel on climate change assessment reports (AR1-AR6). Nat Commun 16(1):6159. <https://doi.org/10.1038/s41467-025-60266-7>
- dos Reis GS, Grimm A, Fungaro DA, Hu T, de Brum IAS, Lima EC, Naushad M, Dotto GL, Lassi U (2024) Synthesis of sustainable mesoporous sulfur-doped biobased carbon with superior performance sodium diclofenac removal: Kinetic, equilibrium, thermodynamic and mechanism. Environ Res 251: 118595. <https://doi.org/10.1016/j.envres.2024.118595>
- Elhenawy SE, Khraishah M, AlMomanani F, Walker G (2020) Metal-organic frameworks as a platform for CO<sub>2</sub> capture and chemical processes: adsorption, membrane separation, catalytic-conversion, and electrochemical reduction of CO<sub>2</sub>. Catalysts 10(11):1293. <https://doi.org/10.3390/catal10111293>
- Elnour AY, Alghyamah AA, Shaikh HM, Poulouse AM, Al-Zahrani SM, Anis A, Al-Wabel MI (2019) Effect of pyrolysis temperature on biochar microstructural evolution, physicochemical characteristics, and its influence on biochar/polypropylene composites. Appl Sci 9(6):1149. <https://doi.org/10.3390/app9061149>
- Fakhar A, Galgo SJC, Canatoy RC, Rafique M, Sarfraz R, Farooque AA, Khan MI (2025) Advancing modified biochar for sustainable agriculture: a comprehensive review on characterization, analysis, and soil performance. Biochar 7(1):8. <https://doi.org/10.1007/s42773-024-00397-0>
- Fang L, Huang T, Lu H, Wu XL, Chen Z, Yang H, Wang S, Tang Z, Li Z, Hu B, Wang X (2023) Biochar-based materials in environmental pollutant elimination, H<sub>2</sub> production and CO<sub>2</sub> capture applications. Biochar 5(1):42. <https://doi.org/10.1007/s42773-023-00237-7>
- Francis JC, Nighojkar A, Kandasubramanian B (2023) Relevance of wood biochar on CO<sub>2</sub> adsorption: a review. Hybrid Advances 3:100056. <https://doi.org/10.1016/j.hybadv.2023.100056>
- Gai X, Wang H, Liu J, Zhai L, Liu S, Ren T, Liu H (2014) Effects of feedstock and pyrolysis temperature on biochar adsorption of ammonium and nitrate. PLoS One 9(12):e113888. <https://doi.org/10.1371/journal.pone.0113888>
- Gao J, Wang H, Liu X, Zhang Z, Fan Z, Suo Y (2025) Regulating CO<sub>2</sub> adsorption performance of lychee seed-based porous carbon materials: insights into oxygen groups and pore structure. Environ Res 284:122245. <https://doi.org/10.1016/j.envres.2025.122245>
- Gao W, Liang S, Wang R, Jiang Q, Zhang Y, Zheng Q, Xie B, Toe CY, Zhu X, Wang J, Huang L, Gao Y, Wang Z, Jo C, Wang Q, Wang L, Liu Y, Louis B, Scott J, Roger A-C, Amal R, He H, Park SE (2020) Industrial carbon dioxide capture and utilization: state of the art and future challenges. Chem Soc Rev 49(23):8584–8686. <https://doi.org/10.1039/D0CS00025F>
- Gargiulo V, Gomis-Berenguer A, Giudicianni P, Ania CO, Ragucci R, Alfè M (2018) Assessing the potential of biochars prepared by steam-assisted slow pyrolysis for CO<sub>2</sub> adsorption and separation. Energy Fuels 32(10):10218–10227. <https://doi.org/10.1021/acs.energyfuels.8b01058>
- Ge C, Lian D, Cui S, Gao J, Lu J (2019) Highly selective CO<sub>2</sub> capture on waste polyurethane foam-based activated carbon. Processes 7(9):592. <https://doi.org/10.3390/pr7090592>
- Ghanbari S, Kamath G (2019) Dynamic simulation and mass transfer study of carbon dioxide capture using biochar and MgO-impregnated activated carbon in a swing adsorption process. Energ Fuel 33(6):5452–5463. <https://doi.org/10.1021/acs.energyfuels.9b00923>
- González AS, Plaza MG, Rubiera F, Pevida C (2013) Sustainable biomass-based carbon adsorbents for post-combustion CO<sub>2</sub> capture. Chem Eng J 230:456–465. <https://doi.org/10.1016/j.cej.2013.06.118>
- González B, Manyà JJ (2020) Activated olive mill waste-based hydrochars as selective adsorbents for CO<sub>2</sub> capture under postcombustion conditions. Chem Eng Process 149:107830. <https://doi.org/10.1016/j.ccep.2020.107830>
- Guo R, Yan L, Rao P, Wang R, Guo X (2020) Nitrogen and sulfur co-doped biochar derived from peanut shell with enhanced adsorption capacity for diethyl phthalate. Environ Pollut 258:113674. <https://doi.org/10.1016/j.envpol.2019.113674>
- Guo S, Li Y, Wang Y, Wang L, Sun Y, Liu L (2022) Recent advances in biochar-based adsorbents for CO<sub>2</sub> capture. Carbon Capture Science & Technology 4:100059. <https://doi.org/10.1016/j.ccsct.2022.100059>
- Guo T, Zhang Y, Geng Y, Chen J, Zhu Z, Bedane AH, Du Y (2023) Surface oxidation modification of nitrogen doping biochar for enhancing CO<sub>2</sub> adsorption. Ind Crops Prod 206:117582. <https://doi.org/10.1016/j.indcrop.2023.117582>
- Haider MIS, Liu G, Yousaf B, Arif M, Aziz K, Ashraf A, Safeer R, Ijaz S, Pikon K (2024) Synergistic interactions and reaction mechanisms of biochar surface functionalities in antibiotics removal from industrial wastewater. Environ Pollut 356:124365. <https://doi.org/10.1016/j.envpol.2024.124365>
- Han J, Zhang L, Zhao B, Qin L, Wang Y, Xing F (2019) The N-doped activated carbon derived from sugarcane bagasse for CO<sub>2</sub> adsorption. Ind Crop Prod 128:290–297. <https://doi.org/10.1016/j.indcrop.2018.11.028>
- Huong PT, Jitae K, Al Tahtamouni TM, Le Minh Tri N, Kim HH, Cho KH, Lee C (2020) Novel activation of peroxymonosulfate by biochar derived from rice husk toward oxidation of organic contaminants in wastewater. J Water Process Eng 33:101037. <https://doi.org/10.1016/j.jwpe.2019.101037>
- Igalavithana AD, Choi SW, Shang J, Hanif A, Dissanayake PD, Tsang DCW, Kwon JH, Lee KB, Ok YS (2020) Carbon dioxide capture in biochar produced from pine sawdust and paper mill sludge: effect of porous structure and surface chemistry. Sci Total Environ 739:139845. <https://doi.org/10.1016/j.scitotenv.2020.139845>

- Igalavithana AD, Lee SE, Lee YH, Tsang DCW, Rinklebe J, Kwon EE, Ok YS (2017) Heavy metal immobilization and microbial community abundance by vegetable waste and pine cone biochar of agricultural soils. *Chemosphere* 174:593–603. <https://doi.org/10.1016/j.chemosphere.2017.01.148>
- Jang E, Choi SW, Lee KB (2019) Effect of carbonization temperature on the physical properties and CO<sub>2</sub> adsorption behavior of petroleum coke-derived porous carbon. *Fuel* 248:85–92. <https://doi.org/10.1016/j.fuel.2019.03.051>
- Ji C, Zhu S, Zhang E, Li W, Liu Y, Zhang W, Su C, Gu Z, Zhang H (2022) Research progress and applications of silica-based aerogels—a bibliometric analysis. *RSC Adv* 12(22):14137–14153. <https://doi.org/10.1039/D2RA01511K>
- Jiang B, Zhang B, Duan X, Xing Y (2024) CO<sub>2</sub> capture by modified clinoptilolite and its regeneration performance. *Int J Coal Sci Technol* 11(1):20. <https://doi.org/10.1007/s40789-023-00661-x>
- Kazemi Shariat Panahi H, Dehghani M, Ok YS, Nizami AS, Khoshnevisan B, Mussatto SI, Aghbashlo M, Tabatabaei M, Lam SS (2020) A comprehensive review of engineered biochar: production, characteristics, and environmental applications. *J Clean Prod* 270:122462. <https://doi.org/10.1016/j.jclepro.2020.122462>
- Khandaker T, Hossain MS, Dhar PK, Rahman MS, Hossain MA, Ahmed MB (2020) Efficacies of carbon-based adsorbents for carbon dioxide capture. *Processes* 8(6):654. <https://doi.org/10.3390/pr8060654>
- Khoshraftar Z, Ghaemi A (2022) Evaluation of pistachio shells as solid wastes to produce activated carbon for CO<sub>2</sub> capture: isotherm, response surface methodology (RSM) and artificial neural network (ANN) modeling. *Current Research in Green and Sustainable Chemistry* 5:100342. <https://doi.org/10.1016/j.crgsc.2022.100342>
- Khoshraftar Z, Ghaemi A (2024) Enhanced carbon dioxide adsorption using lignin-derived and nitrogen-doped porous carbons: a machine learning approaches, RSM and isotherm modeling. *Case Studies in Chemical and Environmental Engineering* 9:100668. <https://doi.org/10.1016/j.cscee.2024.100668>
- Khoshraftar Z, Masoumi H, Ghaemi A (2023) Characterization and evaluation of low-cost biomass-based-AC for CO<sub>2</sub> capture: a review. *Case Studies in Chemical and Environmental Engineering* 8:100373. <https://doi.org/10.1016/j.cscee.2023.100373>
- Kwon KS, Lee HS (2025) Sustainable development of sawdust biochar as a green and promising material for CO<sub>2</sub> capture technologies. *Materials* 18(14):3243. <https://doi.org/10.3390/ma18143243>
- Lahijani P, Mohammadi M, Mohamed AR (2018) Metal incorporated biochar as a potential adsorbent for high capacity CO<sub>2</sub> capture at ambient condition. *J CO<sub>2</sub> Util* 26:281–293. <https://doi.org/10.1016/j.jcou.2018.05.018>
- Lee G, Ahmed I, Jhung SH (2024) CO<sub>2</sub> adsorption using functionalized metal-organic frameworks under low pressure: contribution of functional groups, excluding amines, to adsorption. *Chem Eng J* 481:148440. <https://doi.org/10.1016/j.cej.2023.148440>
- Leng L, Huang H, Li H, Li J, Zhou W (2019) Biochar stability assessment methods: a review. *Sci Total Environ* 647:210–222. <https://doi.org/10.1016/j.scitotenv.2018.07.402>
- León M, Silva J, Carrasco S, Barrientos N (2020) Design, cost estimation and sensitivity analysis for a production process of activated carbon from waste nutshells by physical activation. *Processes* 8(8):945. <https://doi.org/10.3390/pr8080945>
- Li H, Liu J, Zheng H, Wang C, Zhu L, Wang J, Cai J (2026) One-step template-free pyrolysis for biochar: biomass organs control porosity and high-performance for methylene blue removal from water. *Bioresour Technol* 439:133280. <https://doi.org/10.1016/j.biortech.2025.133280>
- Li K, Zhang D, Niu X, Guo H, Yu Y, Tang Z, Lin Z, Fu M (2022a) Insights into CO<sub>2</sub> adsorption on KOH-activated biochars derived from the mixed sewage sludge and pine sawdust. *Sci Total Environ* 826:154133. <https://doi.org/10.1016/j.scitotenv.2022.154133>
- Li M, Xiao R (2019) Preparation of a dual pore structure activated carbon from rice husk char as an adsorbent for CO<sub>2</sub> capture. *Fuel Process Technol* 186:35–39. <https://doi.org/10.1016/j.fuproc.2018.12.015>
- Li N, He M, Lu X, Yan B, Duan X, Chen G, Wang S, La H (2022b) Municipal solid waste derived biochars for wastewater treatment: production, properties and applications. *Resour Conserv Recycl* 177:106003. <https://doi.org/10.1016/j.resconrec.2021.106003>
- Li R, Zhang C, Hui J, Shen T, Zhang Y (2024a) The application of P-modified biochar in wastewater remediation: a state-of-the-art review. *Sci Total Environ* 917:170198. <https://doi.org/10.1016/j.scitotenv.2024.170198>
- Li S, Diao R, Liu X, Qi F, Yang S, Ma P (2024b) Valorization of bio-oil distillation residue through co-pyrolysis with moso bamboo to prepare biochar: optimization study on effects of blend ratio, pyrolysis temperature, and residence time. *J Anal Appl Pyrolysis* 177:106356. <https://doi.org/10.1016/j.jaap.2024.106356>
- Li W, Cui H, Xu J, Shi J (2022c) N-doped porous carbon prepared from filter paper for CO<sub>2</sub> capture. *Chem Phys Lett* 787:139275. <https://doi.org/10.1016/j.cplett.2021.139275>
- Li Z, Tong W, Li C, Dong Z, Han S, Li K, Wang J, Qu J, Zhang Y (2025) Advances on nitrogen-doped biochar for adsorption and degradation of organic pollutants from aquatic environment: mechanisms and applications. *Sep Purif Technol* 354:129017. <https://doi.org/10.1016/j.seppur.2024.129017>
- Liang H, Sun R, Song B, Sun Q, Peng P, She D (2020) Preparation of nitrogen-doped porous carbon material by a hydrothermal-activation two-step method and its high-efficiency adsorption of Cr(VI). *J Hazard Mater* 387:121987. <https://doi.org/10.1016/j.jhazmat.2019.121987>
- Liang H, Zhou X (2024) Mathematical modeling and analysis of atmospheric CO<sub>2</sub> concentration and global temperature change: a multi-model approach. *Highl Sci Eng Technol* 115:458–467. <https://doi.org/10.54097/ehhj9991>
- Lim G, Lee KB, Ham HC (2016) Effect of N-containing functional groups on CO<sub>2</sub> adsorption of carbonaceous materials: a density functional theory approach. *J Phys Chem C* 120(15):8087–8095. <https://doi.org/10.1021/acs.jpcc.5b12090>
- Liu F, Wang Z, Zhang H, Jin L, Chu X, Gu B, Huang H, Yang W (2019a) Nitrogen, oxygen and sulfur co-doped hierarchical porous carbons toward high-performance supercapacitors by direct pyrolysis of kraft lignin. *Carbon* 149:105–116. <https://doi.org/10.1016/j.carbon.2019.04.023>
- Liu H, Zhang F, Wu Z, Cui E, Yue L, Hou G, Wang L (2021) Nitrogen-doped porous carbon derived from cellulose microfibers of rice straw for high-performance electrodes of supercapacitors. *Energy Fuels* 35(12):10190–10198. <https://doi.org/10.1021/acs.energyfuels.1c00323>
- Liu WJ, Jiang H, Yu HQ (2019b) Emerging applications of biochar-based materials for energy storage and conversion. *Energy Environ Sci* 12(6):1751–1779. <https://doi.org/10.1039/C9EE02066E>
- Liu WJ, Li WW, Jiang H, Yu HQ (2017) Fates of chemical elements in biomass during its pyrolysis. *Chem Rev* 117(9):6367–6398. <https://doi.org/10.1021/acs.chemrev.6b00647>
- Liu X, Zhao Y, Ma J, Zhang Y, Zhang H, Liu Z, Liu Y (2025) Defects mediate the active N sites in N-doped carbon catalyst for efficiently catalyzing H<sub>2</sub>S to element sulfur. *Appl Catal B Environ* 380:125718. <https://doi.org/10.1016/j.apcatb.2025.125718>
- Llamas B, Suárez-Rodríguez MC, González-López CV, Mora P, Acién FG (2021) Techno-economic analysis of microalgae related processes for CO<sub>2</sub> bio-fixation. *Algal Res* 57:102339. <https://doi.org/10.1016/j.algal.2021.102339>
- Lu G, Wang Z, Bhatti UH, Fan X (2023) Recent progress in carbon dioxide capture technologies: a review. *Clean Energy Sci Technol* 1(1):1–47. <https://doi.org/10.18686/cest.v1i1.32>
- Luo M, Jiang X, Liu Y, Liu Y, Yu H, Niu Y, Meng X, Wang L, Niu Y (2023) Enhanced adsorption complexation of biochar by nitrogen-containing functional groups. *J Environ Chem Eng* 11(6):111194. <https://doi.org/10.1016/j.jece.2023.111194>
- Ma C, Bai J, Hu X, Jiang Z, Wang L (2023) Nitrogen-doped porous carbons from polyacrylonitrile fiber as effective CO<sub>2</sub> adsorbents. *J Environ Sci (China)* 125:533–543. <https://doi.org/10.1016/j.jes.2022.03.016>
- Manyà JJ, García-Morcate D, González B (2020) Adsorption performance of physically activated biochars for postcombustion CO<sub>2</sub> capture from dry and humid flue gas. *Appl Sci* 10(1):376. <https://doi.org/10.3390/app10010376>
- Manyà JJ, González B, Azuara M, Arner G (2018) Ultra-microporous adsorbents prepared from vine shoots-derived biochar with high CO<sub>2</sub> uptake and CO<sub>2</sub>/N<sub>2</sub> selectivity. *Chem Eng J* 345:631–639. <https://doi.org/10.1016/j.cej.2018.01.092>
- Mochizuki Y, Bud J, Byambajav E, Tsubouchi N (2025) Pore properties and CO<sub>2</sub> adsorption performance of activated carbon prepared from various carbonaceous materials. *Carbon Resour Convers* 8(1):100237. <https://doi.org/10.1016/j.crcon.2024.100237>

- Montes-Morán MA, Suárez D, Menéndez JA, Fuente E (2004) On the nature of basic sites on carbon surfaces: an overview. *Carbon* 42(7):1219–1225. <https://doi.org/10.1016/j.carbon.2004.01.023>
- Mou X, Ma J, Zheng S, Chen X, Krumeich F, Hauert R, Lin R, Wu ZS, Ding Y (2021) A general synthetic strategy toward highly doped pyridinic nitrogen-rich carbons. *Adv Funct Mater* 31(3):2006076. <https://doi.org/10.1002/adfm.202006076>
- Mukhtar A, Saqib B, Mellon NB, Rafiq S, Babar M, Ullah S, Muhammad N, Khan AL, Ayoub M, Ibrahim M, Maqsood K, Bustam MA, Al-Sehemi AG, Klemeš JJ, Asif S, Bokhari A (2020) A review on CO<sub>2</sub> capture via nitrogen-doped porous polymers and catalytic conversion as a feedstock for fuels. *J Clean Prod* 277:123999. <https://doi.org/10.1016/j.jclepro.2020.123999>
- Niu J, Ai P, Guo Q, Jin H, Gao Z, Huang W (2023) The effect of nitrogen doping on hydrogenation capability and stability of Cu-based catalyst in ester hydrogenation to methyl glycolate. *Fuel* 351:128866. <https://doi.org/10.1016/j.fuel.2023.128866>
- Ogungbenro AE, Quang DV, Al-Ali KA, Vega LF, Abu-Zahra MRM (2018) Physical synthesis and characterization of activated carbon from date seeds for CO<sub>2</sub> capture. *J Environ Chem Eng* 6(4):4245–4252. <https://doi.org/10.1016/j.jece.2018.06.030>
- Osman AI, Hefny M, Abdel Maksoud MIA, Elgarahy AM, Rooney DW (2021) Recent advances in carbon capture storage and utilisation technologies: a review. *Environ Chem Lett* 19(2):797–849. <https://doi.org/10.1007/s10311-020-01133-3>
- Ouyang L, Xiao J, Jiang H, Yuan S (2021) Nitrogen-doped porous carbon materials derived from graphene oxide/melamine resin composites for CO<sub>2</sub> adsorption. *Molecules* 26(17):5293. <https://doi.org/10.3390/molecules26175293>
- Pan G, Wei J, Xu M, Li J, Wang L, Li Y, Cui N, Li J, Wang Z (2023) Insight into boron-doped biochar as efficient metal-free catalyst for peroxymonosulfate activation: Important role of -O-B-O- moieties. *J Hazard Mater* 445:130479. <https://doi.org/10.1016/j.jhazmat.2022.130479>
- Park S, Choi MS, Park HS (2019) Nitrogen-doped nanoporous carbons derived from lignin for high CO<sub>2</sub> capacity. *Carbon Lett* 29(3):289–296. <https://doi.org/10.1007/s42823-019-00025-z>
- Petrovic B, Gorbounov M, Masoudi Soltani S (2021) Influence of surface modification on selective CO<sub>2</sub> adsorption: a technical review on mechanisms and methods. *Microporous Mesoporous Mater* 312:110751. <https://doi.org/10.1016/j.micromeso.2020.110751>
- Plaza MG, García S, Rubiera F, Pis JJ, Pevida C (2011) Evaluation of ammonia modified and conventionally activated biomass based carbons as CO<sub>2</sub> adsorbents in postcombustion conditions. *Sep Purif Technol* 80(1):96–104. <https://doi.org/10.1016/j.seppur.2011.04.015>
- Plaza MG, Pevida C, Martín CF, Feroso J, Pis JJ, Rubiera F (2010) Developing almond shell-derived activated carbons as CO<sub>2</sub> adsorbents. *Sep Purif Technol* 71(1):102–106. <https://doi.org/10.1016/j.seppur.2009.11.008>
- Portillo E, Alonso-Fariñas B, Vega F, Cano M, Navarrete B (2019) Alternatives for oxygen-selective membrane systems and their integration into the oxy-fuel combustion process: a review. *Sep Purif Technol* 229:115708. <https://doi.org/10.1016/j.seppur.2019.115708>
- Puziy AM, Poddubnaya OI, Gawdzik B, Tascón JMD (2020) Phosphorus-containing carbons: preparation, properties and utilization. *Carbon* 157:796–846. <https://doi.org/10.1016/j.carbon.2019.10.018>
- Quan C, Su R, Gao N (2020) Preparation of activated biomass carbon from pine sawdust for supercapacitor and CO<sub>2</sub> capture. *Int J Energy Res* 44(6):4335–4351. <https://doi.org/10.1002/er.5206>
- Rangabhashiyam S, Lins P, Oliveira L, Sepulveda P, Ighalo JO, Rajapaksha AU, Meili L (2022) Sewage sludge-derived biochar for the adsorptive removal of wastewater pollutants: a critical review. *Environ Pollut* 293:118581. <https://doi.org/10.1016/j.envpol.2021.118581>
- Rao L, Liu S, Wang L, Ma C, Wu J, An L, Hu X (2019) N-doped porous carbons from low-temperature and single-step sodium amide activation of carbonized water chestnut shell with excellent CO<sub>2</sub> capture performance. *Chem Eng J* (1996) 359:428–435. <https://doi.org/10.1016/j.cej.2018.11.065>
- Rashidi NA, Yusup S (2020) Biochar as potential precursors for activated carbon production: parametric analysis and multi-response optimization. *Environ Sci Pollut Res Int* 27(22):27480–27490. <https://doi.org/10.1007/s11356-019-07448-1>
- Razzak SA (2024) Municipal solid and plastic waste derived high-performance biochar production: a comprehensive review. *J Anal Appl Pyrolysis* 181:106622. <https://doi.org/10.1016/j.jaap.2024.106622>
- Ruen-ngam D, Doungmanee R, Ronbanchob A, Pavasant P (2009) Zeolite formation from coal fly ash and its adsorption potential. *J Air Waste Manag Assoc* 59(10):1140–1147. <https://doi.org/10.3155/1047-3289.59.10.1140>
- Saha D, Kienbaum MJ (2019) Role of oxygen, nitrogen and sulfur functionalities on the surface of nanoporous carbons in CO<sub>2</sub> adsorption: a critical review. *Microporous Mesoporous Mater* 287:29–55. <https://doi.org/10.1016/j.micromeso.2019.05.051>
- Sai Bhargava Reddy M, Ponnamma D, Sadasivuni KK, Kumar B, Abdullah AM (2021) Carbon dioxide adsorption based on porous materials. *RSC Adv* 11(21):12658–12681. <https://doi.org/10.1039/D0RA10902A>
- Sajjadi B, Chen WY, Egiebor NO (2019) A comprehensive review on physical activation of biochar for energy and environmental applications. *Rev Chem Eng* 35(6):735–776. <https://doi.org/10.1515/revce-2017-0113>
- Salimi P, Verduyck W, Chauque S, Yari S, Venezia E, Lataf A, Ghanemnia N, Zafar MS Safari M, Hardy A, Proietti Zaccaria R, Vandamme D (2024) Lithium-metal-free sulfur batteries with biochar and steam-activated biochar-based anodes from spent common ivy. *Energy Environ Mater* 7(6):1–11. <https://doi.org/10.1002/eem2.12758>
- Sánta R, Garbai L (2025) Investigation of the dynamic equilibrium of atmospheric CO<sub>2</sub> concentrations. *Air Qual Atmos Health* 18(9):2655–2667. <https://doi.org/10.1007/s11869-025-01783-8>
- Schnieder B, Schmid R, Hättig C (2025) Quantum chemical study on the evolution of sulfur functional groups during char burnout. *J Phys Chem A* 129(14):3300–3314. <https://doi.org/10.1021/acs.jpca.4c07973>
- Schroeder J, Neomagus HWJP, Bunt JR, Everson RC, Uwamao RC (2024) Steam gasification kinetics of biochar at elevated pressures. *Heliyon* 10(11):e31172. <https://doi.org/10.1016/j.heliyon.2024.e31172>
- Senthilkumar M, Saravanan C, Sethuraman V, Puthiaraj P, Muthu Mareeswaran P (2020) Nitrogen-rich polyaminal porous network for CO<sub>2</sub> uptake studies and preparation of carbonized materials. *Eur Polym J* 124:109477. <https://doi.org/10.1016/j.eurpolymj.2020.109477>
- Shafawi AN, Mohamed AR, Lahijani P, Mohammadi M (2021) Recent advances in developing engineered biochar for CO<sub>2</sub> capture: an insight into the biochar modification approaches. *J Environ Chem Eng* 9(6):106869. <https://doi.org/10.1016/j.jece.2021.106869>
- Shahkarami S, Azargohar R, Dalai AK, Soltan J (2015) Breakthrough CO<sub>2</sub> adsorption in bio-based activated carbons. *J Environ Sci* 34:68–76. <https://doi.org/10.1016/j.jes.2015.03.008>
- Shao J, Ma C, Zhao J, Wang L, Hu X (2022) Effective nitrogen and sulfur co-doped porous carbonaceous CO<sub>2</sub> adsorbents derived from amino acid. *Colloid Surf A Physicochem Eng Asp* 632:127750. <https://doi.org/10.1016/j.colsurfa.2021.127750>
- Shao J, Wang Y, Che M, Xiao Q, Demir M, Al Mesfer MK, Wang L, Hu X, Liu Y (2025) N, S co-doped porous carbons from coconut shell for selective CO<sub>2</sub> adsorption. *J Energy Inst* 123:102273. <https://doi.org/10.1016/j.joei.2025.102273>
- Shi J, Yan N, Cui H, Liu Y, Weng Y (2017a) Sulfur doped microporous carbons for CO<sub>2</sub> adsorption. *J Environ Chem Eng* 5(5):4605–4611. <https://doi.org/10.1016/j.jece.2017.09.002>
- Shi J, Yan N, Cui H, Liu Y, Weng Y, Li D, Ji X (2017b) Nitrogen doped hierarchically porous carbon derived from glucosamine hydrochloride for CO<sub>2</sub> adsorption. *J CO<sub>2</sub> Util* 21:444–449. <https://doi.org/10.1016/j.jcou.2017.08.010>
- Shi R, Liu K, Liu B, Chen H, Xu X, Ren Y, Qiu J, Zeng Z, Li L (2022) New insight into toluene adsorption mechanism of melamine urea-formaldehyde resin based porous carbon: experiment and theory calculation. *Colloid Surf A Physicochem Eng Asp* 632:127600. <https://doi.org/10.1016/j.colsurfa.2021.127600>
- Shinde PA, Shrestha LK, Ariga K (2025) Heteroatom-functionalized carbon nanoarchitectonics: unlocking the doping effects for supercapacitor electrode design. *Green Energy Environ* 10(9):1838–1862. <https://doi.org/10.1016/j.gee.2025.02.007>
- Sierra-Jimenez V, Macías RJ, Mathews JP, Carré V, Leclerc S, Budai A, Chejne F, Castro-Gutiérrez J, Celzard A, Fierro V, García-Pérez M (2025) Influence of acid-catalyzed dehydration and pressure on woody biomass carbonization: exploring carbon yield, heteroatom functionalities, and biochar atomistic structure. *Carbon* 242:120474. <https://doi.org/10.1016/j.carbon.2025.120474>

- Singh Karam D, Nagabovanalli P, Sundara Rajoo K, Fauziah Ishak C, Abdu A, Rosli Z, Melissa Muharam F, Zulperi D (2022) An overview on the preparation of rice husk biochar, factors affecting its properties, and its agriculture application. *J Saudi Soc Agric Sci* 21(3):149–159. <https://doi.org/10.1016/j.jssas.2021.07.005>
- Sui L, Tang C, Du Q, Zhao Y, Cheng K, Yang F (2021) Preparation and characterization of boron-doped corn straw biochar: Fe (III) removal equilibrium and kinetics. *J Environ Sci* 106:116–123. <https://doi.org/10.1016/j.jes.2021.01.001>
- Sun LM, McIntyre SR, Iacomì P, Everden K, Williams PT, Zong S, Liu X, Zhu X, Yang Y, Li S, Wu G, Huang F, Liu L, Yuan X, Zhang H, Zhang J, Yang H, Chen W, Sun H, Cao Y, Feng D, Cheng Z, Zhang X, Liang D, Liu S, Zhang X, Zhu X, Zhang YS, Yan Y, Zha J, Qiao Y, Soltani SM, Zhang N, Yi S, Wu C (2025) Biochar production, activation, and applications: a comprehensive technical review. *Carbon Capture Science & Technology* 16:100421. <https://doi.org/10.1016/j.ccs.2025.100421>
- Sun Y, Jia J, Huo L, Zhao L, Yao Z, Liu Z (2024) Heteroatom-doped biochar for CO<sub>2</sub> adsorption: a review of heteroatoms, doping methods, and functions. *Biomass Convers Bior* 14(14):15237–15249. <https://doi.org/10.1007/s13399-022-03640-5>
- Sun Y, Jia J, Huo LW, Zhao L, Yao Z, Liu Z (2023a) Heteroatom-doped biochar for CO<sub>2</sub> adsorption: a review of heteroatoms, doping methods, and functions. *Biomass Convers Bior* 1–13. <https://doi.org/10.1007/s13399-022-03640-5>
- Sun Y, Jia J, Liu Z, Liu Z, Huo L, Zhao L, Zhao Y, Yao Z (2023b) Heteroatom-doped biochar devised from cellulose for CO<sub>2</sub> adsorption: a new vision on competitive behavior and interactions of N and S. *Biochar* 5(1):76. <https://doi.org/10.1007/s42773-023-00275-1>
- Suo F, You X, Ma Y, Li Y (2019) Rapid removal of triazine pesticides by P doped biochar and the adsorption mechanism. *Chemosphere* 235:918–925. <https://doi.org/10.1016/j.chemosphere.2019.06.158>
- Tang Z, Gao J, Dong H, Du Q, Feng D, Cheng J, Li J, Peng Y, Zhang T, Xie M, Chen H (2024) Targeted construction of porous biochar with well-developed pore structure for high-performance CO<sub>2</sub> adsorption. *J Environ Chem Eng* 12(6):114182. <https://doi.org/10.1016/j.jece.2024.114182>
- Tiyawate A, Khongtor N, Serafin J, Chaemchuen S, Klomklang N (2024) Combined experimental and grand canonical Monte Carlo simulation study of CO<sub>2</sub> capture in nitrogen and sulfur co-doped biochar derived from biowaste: cost analysis, kinetics, and equilibrium. *J Environ Chem Eng* 12(5):113991. <https://doi.org/10.1016/j.jece.2024.113991>
- Velepini T, Pillay K (2019) Sulphur functionalized materials for Hg(II) adsorption: a review. *J Environ Chem Eng* 7(5):103350. <https://doi.org/10.1016/j.jece.2019.103350>
- Wang C, Jia L, Jin Y, Qin S (2024a) Study on regeneration mechanism of composite adsorbent by Mg-MOF-74-based modified biochar. *Sci Total Environ* 946:173944. <https://doi.org/10.1016/j.scitotenv.2024.173944>
- Wang C, Kou L, Li C, Xu B, Wu Y (2025a) Enhanced degradation of phenol in aqueous solution via persulfate activation by sulfur-doped biochar: insights into catalytic mechanisms and structural properties. *Nanomaterials* 15(13):979. <https://doi.org/10.3390/nano15130979>
- Wang H, Teng H, Wang X, Xu J, Sheng L (2022a) Physicochemical modification of corn straw biochar to improve performance and its application of constructed wetland substrate to treat city tail water. *J Environ Manage* 310:114758. <https://doi.org/10.1016/j.jenvman.2022.114758>
- Wang H, Wang H, Liu G, Yan Q (2021) In-situ pyrolysis of Taihu blue algae biomass as appealing porous carbon adsorbent for CO<sub>2</sub> capture: role of the intrinsic N. *Sci Total Environ* 771:145424. <https://doi.org/10.1016/j.scitotenv.2021.145424>
- Wang J, Lou F, Zhang M, Yuan J (2025b) Recent progress in nitrogen-doped activated carbon: microstructural regulation and enhanced gas adsorption. *J Environ Chem Eng* 13(5):118107. <https://doi.org/10.1016/j.jece.2025.118107>
- Wang J, Wang Y, Liu X, Xiao Q, Demir M, Almesfer MK, Colak SG, Wang L, Hu X, Liu Y (2025c) The synthesis of B-doped porous carbons via a sodium metaborate tetrahydrate activating agent: a novel approach for CO<sub>2</sub> adsorption. *Molecules* 30:2564. <https://doi.org/10.3390/molecules30122564>
- Wang J, Yin Y, Liu X, Liu Y, Xiao Q, Zhao L, Demir M, Alaş Çolak MÖ, Wang L, Hu X (2025d) Potassium metaborate-activated boron-doped porous carbons for selective CO<sub>2</sub> adsorption. *Sep Purif Technol* 376:134079. <https://doi.org/10.1016/j.seppur.2025.134079>
- Wang P, Liu X, Yu B, Wu X, Xu J, Dong F, Zheng Y (2020a) Characterization of peanut-shell biochar and the mechanisms underlying its sorption for atrazine and nicosulfuron in aqueous solution. *Sci Total Environ* 702:134767. <https://doi.org/10.1016/j.scitotenv.2019.134767>
- Wang XF, Xiong L, Li L, Zhong JJ (2020b) Effect of heat treatment temperature on CO<sub>2</sub> capture of nitrogen-enriched porous carbon fibers. *Greenhouse Gases Sci Technol* 10(2):461–471. <https://doi.org/10.1002/ghg.1904>
- Wang Y, Xiao J, Wang H, Zhang TC, Yuan S (2022b) Binary doping of nitrogen and phosphorus into porous carbon: a novel di-functional material for enhancing CO<sub>2</sub> capture and super-capacitance. *J Mater Sci Technol* 99:73–81. <https://doi.org/10.1016/j.jmst.2021.05.035>
- Wang Y, Yan Y, He C, Feng Y, Darma A, Yang J (2024b) The immobilization of cadmium by rape straw derived biochar in alkaline conditions: sorption isotherm, molecular binding mechanism, and in-situ remediation of Cd-contaminated soil. *Environ Pollut* 351:123969. <https://doi.org/10.1016/j.envpol.2024.123969>
- Wang Z, Guo S, Chen G, Zhang M, Sun T, Wang Q, Zhu H, Yang S, Chen Y, Wu M, Lei T, Burra KG, Gupta AK (2024c) Co-pyrolysis of waste tire with agricultural and forestry residues: pyrolysis behavior, products distribution and synergistic effects. *J Energy Inst* 114:101634. <https://doi.org/10.1016/j.joei.2024.101634>
- Wei H, Chen H, Fu N, Chen J, Lan G, Qian W, Liu Y, Lin H, Han S (2017) Excellent electrochemical properties and large CO<sub>2</sub> capture of nitrogen-doped activated porous carbon synthesised from waste longan shells. *Electrochim Acta* 231:403–411. <https://doi.org/10.1016/j.electacta.2017.01.194>
- Wu C, Shi L, Xue S, Li W, Jiang X, Rajendran M, Qian Z (2019) Effect of sulfur-iron modified biochar on the available cadmium and bacterial community structure in contaminated soils. *Sci Total Environ* 647:1158–1168. <https://doi.org/10.1016/j.scitotenv.2018.08.087>
- Wu P, Wang Y, Liu Y (2024a) Recent advances in heteroatom-doped porous carbon for adsorption of gaseous pollutants. *Chem Eng J* 491:152142. <https://doi.org/10.1016/j.cej.2024.152142>
- Wu Q, Zhang Y, Cui MH, Liu H, Liu H, Zheng Z, Zheng W, Zhang C, Wen D (2022a) Pyrolyzing pharmaceutical sludge to biochar as an efficient adsorbent for deep removal of fluoroquinolone antibiotics from pharmaceutical wastewater: performance and mechanism. *J Hazard Mater* 426:127798. <https://doi.org/10.1016/j.jhazmat.2021.127798>
- Wu R, Hang Y, Li J, Bao A (2022b) Preparation of biomass-derived phosphorus-doped microporous carbon material and its application in dye adsorption and CO<sub>2</sub> capture. *Surf Interface Anal* 54(8):881–891. <https://doi.org/10.1002/sia.7101>
- Wu W, Wu C, Liu J, Yan H, Zhang G, Li G, Zhao Y, Wang Y (2024b) Nitrogen-doped porous carbon through K<sub>2</sub>CO<sub>3</sub>-activated bamboo shoot shell for an efficient CO<sub>2</sub> adsorption. *Fuel* 363:130937. <https://doi.org/10.1016/j.fuel.2024.130937>
- Xiao J, Wang Y, Zhang TC, Yuan S (2021) N, S-containing polycondensate-derived porous carbon materials for superior CO<sub>2</sub> adsorption and supercapacitor. *Appl Surf Sci* 562:150128. <https://doi.org/10.1016/j.apsusc.2021.150128>
- Xiong Z, Shihong Z, Haiping Y, Tao S, Yingquan C, Hanping C (2013) Influence of NH<sub>3</sub>/CO<sub>2</sub> modification on the characteristic of biochar and the CO<sub>2</sub> capture. *Bioenergy Res* 6(4):1147–1153. <https://doi.org/10.1007/s12155-013-9304-9>
- Xu X, Xu Z, Gao B, Zhao L, Zheng Y, Huang J, Tsang DCW, Ok YS, Cao X (2020) New insights into CO<sub>2</sub> sorption on biochar/Fe oxyhydroxide composites: kinetics, mechanisms, and in situ characterization. *Chem Eng J* 384:123289. <https://doi.org/10.1016/j.cej.2019.123289>
- Yan L, Weishi G, Nan Z, Changqing Y, Yang Y (2022) Preparation and characterization of wheat straw biochar loaded with aluminium/lanthanum hydroxides: a novel adsorbent for removing fluoride from drinking water. *Environ Technol* 43(18):2771–2784. <https://doi.org/10.1080/09593330.2021.1903563>
- Yang C, Zhao T, Pan H, Liu F, Cao J, Lin Q (2022) Facile preparation of N-doped porous carbon from chitosan and NaNH<sub>2</sub> for CO<sub>2</sub> adsorption and conversion. *Chem Eng J* 432:134347. <https://doi.org/10.1016/j.cej.2021.134347>
- Yang H, Lee CG, Lee J (2023) Utilizing animal manure-derived biochar in catalytic advanced oxidation processes: a review. *J Water Process Eng* 56:104545. <https://doi.org/10.1016/j.jwpe.2023.104545>

- Yang X, Wan Y, Zheng Y, He F, Yu Z, Huang J, Wang H, Ok YS, Jiang Y, Gao B (2019) Surface functional groups of carbon-based adsorbents and their roles in the removal of heavy metals from aqueous solutions: a critical review. *Chem Eng J* 366:608–621. <https://doi.org/10.1016/j.cej.2019.02.119>
- Yang Z, Li Q, Li B, Yan T, Yu S, Qiao Z (2025) COF-999: a high-performance CO<sub>2</sub> adsorbent for direct air capture technology. *Green Carbon* 3:395–397. <https://doi.org/10.1016/j.greenca.2025.03.004>
- Yu J, Liu X, Millan M (2023) A study on pyrolysis of wood of different sizes at various temperatures and pressures. *Fuel* 342:127846. <https://doi.org/10.1016/j.fuel.2023.127846>
- Yuan X, Suvarna M, Lim JY, Pérez-Ramírez J, Wang X, Ok YS (2024) Active learning-based guided synthesis of engineered biochar for CO<sub>2</sub> capture. *Environ Sci Technol* 58(15):6628–6636. <https://doi.org/10.1021/acs.est.3c10922>
- Yuan X, Xiao J, Yilmaz M, Zhang TC, Yuan S (2022) N, P co-doped porous biochar derived from cornstalk for high performance CO<sub>2</sub> adsorption and electrochemical energy storage. *Sep Purif Technol* 299:121719. <https://doi.org/10.1016/j.seppur.2022.121719>
- Zhang H, Jiang F, Zhang X, Hu S, Li J, Zhang H, Liu K (2025a) CO<sub>2</sub> adsorption performance of nitrogen-doped activated carbon from banana pseudo-stem by urea-assisted high-pressure CO<sub>2</sub>-hydrothermal treatment. *Sep Purif Technol* 366:132773. <https://doi.org/10.1016/j.seppur.2025.132773>
- Zhang H, Wang T, Sui Z, Zhang Y, Sun B, Pan WP (2019) Enhanced mercury removal by transplanting sulfur-containing functional groups to biochar through plasma. *Fuel* 253:703–712. <https://doi.org/10.1016/j.fuel.2019.05.068>
- Zhang J, Li G, Zhang S, Shao J, Zhang X, Zhang S, Yang H, Chen H (2025b) Controlled synthesis of biochar with flower-like morphology for CO<sub>2</sub> adsorption: enrichment and efficient accessibility of N-containing sites. *ACS Appl Mater Interfaces* 17(4):6742–6754. <https://doi.org/10.1021/acscami.4c18377>
- Zhang J, Yang M, Zhao W, Zhang J, Zang L (2021) Biohydrogen production amended with nitrogen-doped biochar. *Energy Fuels* 35(2):1476–1487. <https://doi.org/10.1021/acs.energyfuels.0c03405>
- Zhang L, Liu R, Lin R, Wang L, Wang Y, Zhu N (2025c) Preparation and CO<sub>2</sub> adsorption performance of the B-Cu co doping walnut shell biochar. *Energy Fuels* 39(22):10452–10464. <https://doi.org/10.1021/acs.energyfuels.5c00858>
- Zhang X, Wu J, Yang H, Shao J, Wang X, Chen Y, Zhang S, Chen H (2016) Preparation of nitrogen-doped microporous modified biochar by high temperature CO<sub>2</sub>-NH<sub>3</sub> treatment for CO<sub>2</sub> adsorption: effects of temperature. *RSC Adv* 6(100):98157–98166. <https://doi.org/10.1039/C6RA23748G>
- Zhang Z, Zhao Y, Wang T (2020) Spirulina hydrothermal carbonization: effect on hydrochar properties and sulfur transformation. *Bioresour Technol* 306:123148. <https://doi.org/10.1016/j.biortech.2020.123148>
- Zhi Y, Shao J, Liu C, Xiao Q, Demir M, Al Mesfer MK, Danish M, Wang L, Hu X (2025a) High-performance CO<sub>2</sub> adsorption with P-doped porous carbons from lotus petiole biomass. *Sep Purif Technol* 361:131253. <https://doi.org/10.1016/j.seppur.2024.131253>
- Zhi Y, Shao J, Wang J, Liu X, Xiao Q, Demir M, Simsek UB, Wang L, Hu X (2025b) Novel synthesis of phosphorus-doped porous carbons from Lotus Petiole using sodium phytate for selective CO<sub>2</sub> capture. *Molecules* 30:3990. <https://doi.org/10.3390/molecules301939902025>
- Zhi Y, Yin Y, Ciren Q, Xiao Q, Zhao L, Demir M, Simsek UB, Hu X, Wang L (2025c) One-step synthesis of K<sub>3</sub>PO<sub>4</sub>-activated phosphorus-enriched carbons for enhanced carbon capture. *J Environ Chem Eng* 13(3):116694. <https://doi.org/10.1016/j.jece.2025.116694>
- Zhou Y, Wang J, Sun M, Li W, Hu X (2021) Adsorption of CO<sub>2</sub> by nitrogen doped corn straw based biochar. *Arab J Geosci* 14(18):1875. <https://doi.org/10.1007/s12517-021-08224-7>
- Zubbri NA, Mohamed AR, Kamiuchi N, Mohammadi M (2020) Enhancement of CO<sub>2</sub> adsorption on biochar sorbent modified by metal incorporation. *Environ Sci Pollut Res* 27(11):11809–11829. <https://doi.org/10.1007/s11356-020-07734-3>
- Zubbri NA, Mohamed AR, Lahijani P, Mohammadi M (2021) Low temperature CO<sub>2</sub> capture on biomass-derived KOH-activated hydrochar established through hydrothermal carbonization with water-soaking pre-treatment. *J Environ Chem Eng* 9(2):105074. <https://doi.org/10.1016/j.jece.2021.105074>

## Publisher's Note

Springer Nature remains neutral with regard to jurisdictional claims in published maps and institutional affiliations.